



3 1176 00167 7682

NASACR-164,027

(NASA-CR-164027) PRELIMINARY DESIGN OF A
SUPERCONDUCTING COIL ARRAY FOR NASA
PROTOTYPE MAGNETIC BALANCE M.S. Thesis
(Massachusetts Inst. of Tech.) 67 p
HC A04/MF A04

N81-18064

Unclas
12047

CSCS 14B G3/09

PRELIMINARY DESIGN OF A
SUPERCONDUCTING COIL ARRAY FOR
NASA PROTOTYPE MAGNETIC BALANCE

by

Mohammad M. Alishahi

Course XVI

S.M.

May, 1980

NASA-CR-164027

19810009540



NF01738

NSG-1356

PRELIMINARY DESIGN OF A SUPERCONDUCTING
COIL ARRAY FOR NASA PROTOTYPE MAGNETIC BALANCE

by

Mohammad M. Alishahi

B.S., Tehran University of Technology (1978)

SUBMITTED IN PARTIAL FULFILLMENT
OF THE REQUIREMENTS FOR THE
DEGREE OF MASTER OF SCIENCE

LIBRARY COPY

at the

MAY 28 1981

LANGLEY RESEARCH CENTER
LIBRARY, NASA
HAMPTON, VIRGINIA

MASSACHUSETTS INSTITUTE OF TECHNOLOGY

May, 1980

Signature of Author

Mohammad M. Alishahi

Department of

Aeronautics and Astronautics

May, 1980

Certified by

Chas. W. Holden

Thesis Supervisor

Accepted by

Chairman, Departmental Graduate Committee

PRELIMINARY DESIGN OF A SUPERCONDUCTING
COIL ARRAY FOR NASA PROTOTYPE MAGNETIC BALANCE

by

Mohammad M. Alishahi

Submitted to the Department of
Aeronautics and Astronautics on May 9, 1980
in partial fulfillment of the requirements for
the degree of Master of Science.

ABSTRACT

Using a computer program a partly optimized configuration for a superconducting version of side and lift coil system of NASA-MIT prototype is presented. Cable size for the mentioned coils and also for superconducting drag and magnetizing coils regarding the overall computed field is determined.

Thesis Supervisor: Charles W. Haldeman
Title: Principal Research Engineer

ACKNOWLEDGEMENTS

The research for this thesis was supported by Grant NSG 1356 from the NASA Langley Research Center. I must acknowledge the constant help and encouragement from Dr. Charles W. Haldeman, and Professor Morton Finston. The accomplishment of this research was made possible through craftsmanship of Mr. Carlo Guidetti. I must also thank Ms. Pat McSweeney, who typed this manuscript.

TABLE OF CONTENTS

<u>Chapter Number</u>		<u>Page Number</u>
I	INTRODUCTION	9
	1.1 Magnetic Balances	9
	1.2 Superconductivity	10
	1.3 The Problem at Hand	10
II	THEORY	12
	2.1 Basic Properties	12
	2.2 Superconductors	14
	2.3 Penetration Depth and Hysteresis Losses	17
III	DESIGN	20
	3.1 The Magnetic Suspension and Balance System	20
	3.2 The Computer Program	23
	3.3 Testing Computer Program	26
	3.4 Finding the Best Configuration	26
	3.5 Magnetizing and Drag Coils	35
	3.6 Magnetic Field Inside Coils and the Conductor Size	38
IV	DISCUSSION	51
	4.1 Discussion	51
Appendix 1	Convergence of Computer Results	53
2	Computer Program TABLE and Computer Results	55

References

LIST OF TABLES

<u>Table Number</u>		<u>Page Number</u>
1	Gradient of Different Stages of a Side and Lift Coil Model	34
2	Maximum Magnetic Field Inside Coils with Percentage of Contribution of each Set	43
3	Final Cable Dimension for Different Coils	50

LIST OF FIGURES

<u>Figure Number</u>		<u>Page Number</u>
1	Variation of the Inside vs Outside Field for a Superconductor and a Perfect Conductor	13
2	Magnetization and Resistance vs. External Field for a Type I Superconductor	15
3	Magnetization and Resistance vs. External Field for a Type II Superconductor	16
4	Typical Current Density Relation vs. Transverse Magnetic Field for a Type II Superconductor Alloy	18
5	Assembly of Magnet System	21
6	Side and Lift Coil Assembly	22
7	Free Space for Design	24
8	Sample Coil Geometry Specifications	25
9	Model Coil	27
10	Comparison of Computer and Test Results	28
11	Model I	30
12	Model II Specifications	31
13	Model III	32
14	Designed Side and Lift Coil Results	36
15	Designed Magnetizing Coil Results	39
16	Designed Drag Coil Results	40

LIST OF FIGURES (continued)

<u>Figure Number</u>		<u>Page Number</u>
17	Assembly of Designed Coils	41
18	Field Magnitude Inside Side and Lift Coil First Stage	44
19	Field Magnitude Inside Side and Lift Coil Second Stage	45
20	Field Magnitude Inside Drag Coil	46
21	Field Magnitude Inside Magnetizing Coil	47
22	Convergence Characteristic of Computer Program TABLE	54

LIST OF SYMBOLS

B	Magnetic induction
B_p	Filament penetration field from London model
$B_{x,y,z}$	Applied magnetic field intensity in the "x", "y", "z" direction
\bar{B}_{xx}	Average value of $\partial B_x / \partial x$
\bar{B}_{yx}	Average value of $\partial B_y / \partial x$
\bar{B}_{zx}	Average value of $\partial B_z / \partial x$
H_c	Critical field strength for superconductivity
H_{c1}	Lower critical field strength for Type II superconductor
H_{c2}	Upper critical field strength for Type II superconductor
I_x	Magnetizing coil current
I_{xx}	Drag coil current
I_{zx}	"Lift force" current
J	Current density
J_c	Critical current density
M	Number of layers in a winding
N	Number of turns per layer

LIST OF SYMBOLS (continued)

Nb_3Sn	Niobium-Tin compound
NbTi	Niobium-Titanium alloy
NbZr	Niobium-Zirconium alloy
μ_0	Permeability of free space

Chapter I

INTRODUCTION

1.1 Magnetic Balances

Magnetic suspension of models in wind tunnels is more advantageous than conventional support of models for two reasons: first, it has no effect on the flow and secondly, it provides the capability to perform dynamic stability tests.

Since magnetic suspension of models in large wind tunnels with high dynamic pressure, such as NASA 1 ft² pilot cryogenic wind tunnel, requires high fields, using a superconducting magnetic balance would reduce the required power.

Investigation of using superconducting coils for magnetic suspension and balance systems has been done at the M.I.T. Aerophysics Laboratory in three parts: first, Kraemer (1) studied low A.C. losses and found the type of superconducting wire that had acceptably low losses. Secondly, Prey (2) performed some experiments on A.C. losses in interacting superconducting magnetic coils. This thesis tries to design a superconducting coil array for present side force, lift, drag and magnetizing coils

of the NASA prototype magnetic suspension and balance system. So, it provides a preview of full design procedure for such a system.

1.2 Superconductivity

It is well known that superconductivity is the absence of electrical resistance due to interaction between electron pairs and the crystal lattice of superconducting material.

Superconductivity can be extinguished by disturbing the electron pairs, such as increasing temperature, which results in lattice vibration or by an external magnetic field which causes internal voltage difference and accelerates the electrons.

There are two types of superconductors:

Type I, pure materials, which have zero resistance to direct current but cannot retain superconductivity in the presence of an external magnetic field.

Type II, superconductors, metallic compounds and alloys, are more suitable for M.S.B. systems because they can tolerate magnetic fields to some extent.

1.3 The Problem at Hand

It was shown in (1) that a suitable conductor for an M.S.B. system capable of dynamic suspension of models is a cable of fully transposed fine copper wires,

each having a single superconducting core and all wires being electrically insulated from each other.

The interacting coil losses using the mentioned kind of superconductor was studied in (2) and it was shown that the interacting losses are about 10-15% of self field coil losses.

The basic approach to the design of a superconducting coil array for the M.S.B. that has been followed in this work consists of these steps: First, developing a computer program to compute the field due to different coil geometry (straight line or circular current element) and then using this to find the best coil configuration, which produces the desired field. This minimizes the superconducting volume and as a result, reduces the overall losses. Secondly, computing the field at several wire locations inside the coils to determine the minimum superconductor cable size.

Chapter II

THEORY

2.1 Basic Properties

A basic property of superconductivity which has direct benefit in engineering is the absence of electrical resistance to direct current. A more important aspect is the Meissner effect, which is the main difference between a superconductor and a perfect conductor. Figure 1 shows this effect; after increasing the field above H_c , the field inside the superconductor jumps to H_c with the loss of superconductivity. Upon decreasing the external field the inside field again returns to zero upon reaching H_c no matter what the history of the process was. In this regard superconductivity is a reversible phenomenon. In contrast to this is a perfect conductor, which retains its inside field after passing H_c and decreasing the field; i.e., a superconductor expells all fields as long as it is superconducting whereas a perfect conductor could have fields frozen in by the onset of perfect condition.

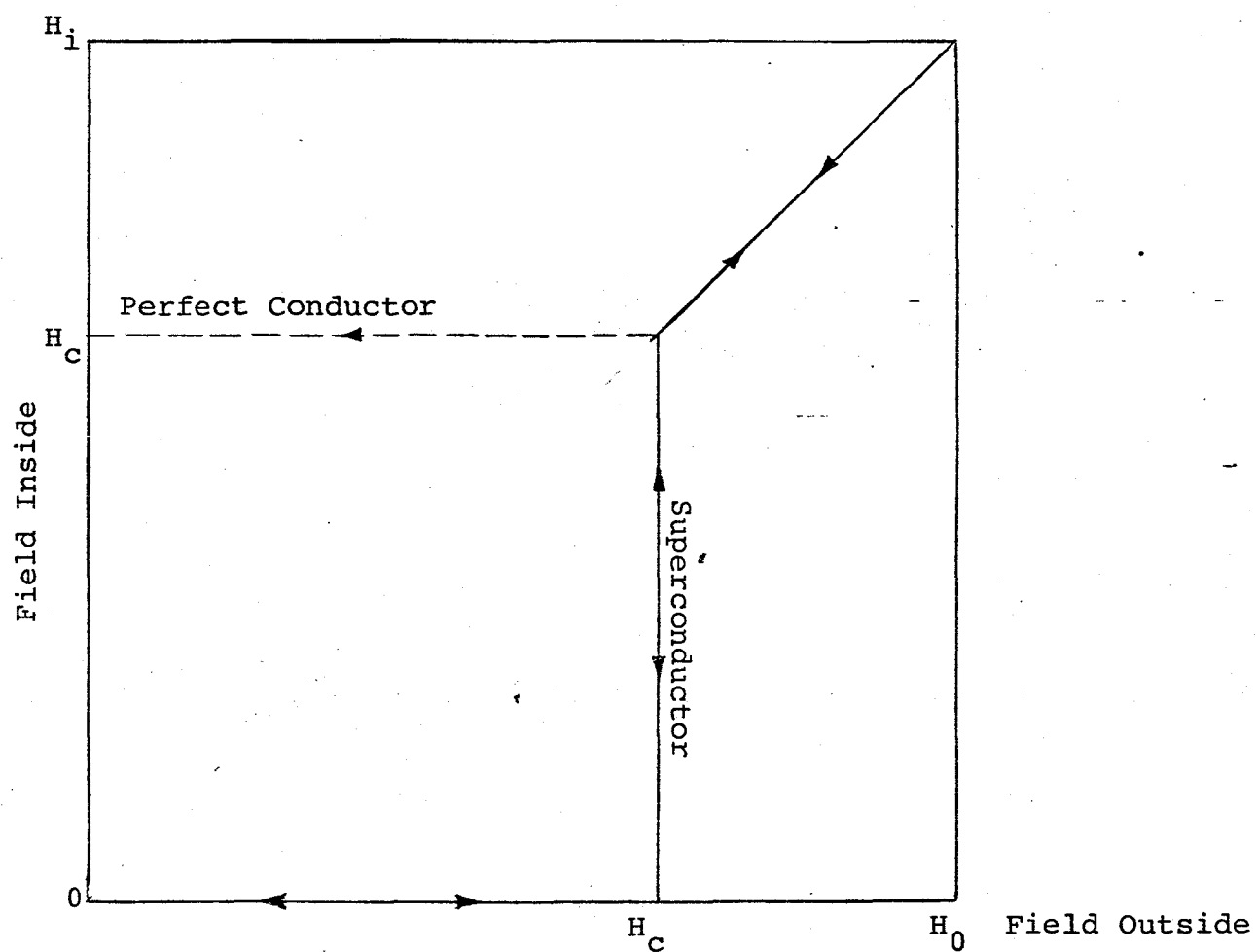


Figure 1. Variation of the Inside vs Outside Field for a Superconductor and a Perfect Conductor, which both have a critical field H_c .

2.2 Superconductors

a) Type I superconductors have a magnetization vs. external field, as shown in Figure 2. There is one critical field for them at which both Meissner and resistive transition occur. However, superconductivity in Type I is extinguished by a field of the order of .1 Tesla or less. So they cannot be used in the proposed M.S.B. Lead and Niobium are among Type I materials.

b) Type II superconductors are known with two critical fields H_{c1} and H_{c2} (Figure 3). At fields less than H_{c1} there is no flux inside the superconductor. Between H_{c1} and H_{c2} flux penetrates in a small depth. The rest of the conductor remains in superconducting state.

If Type II superconductors had no imperfections and grain boundaries as low energy sites for this penetrated flux (fluxio), fluxios would move due to Lorentz forces and dissipate energy. Fortunately, by heat treatment different grain boundaries are produced and as a result high pinning strengths are attainable. Most interesting engineering superconductors are of Type II. They include metallic compounds and alloys, such as NbTi Niobium-Titanium

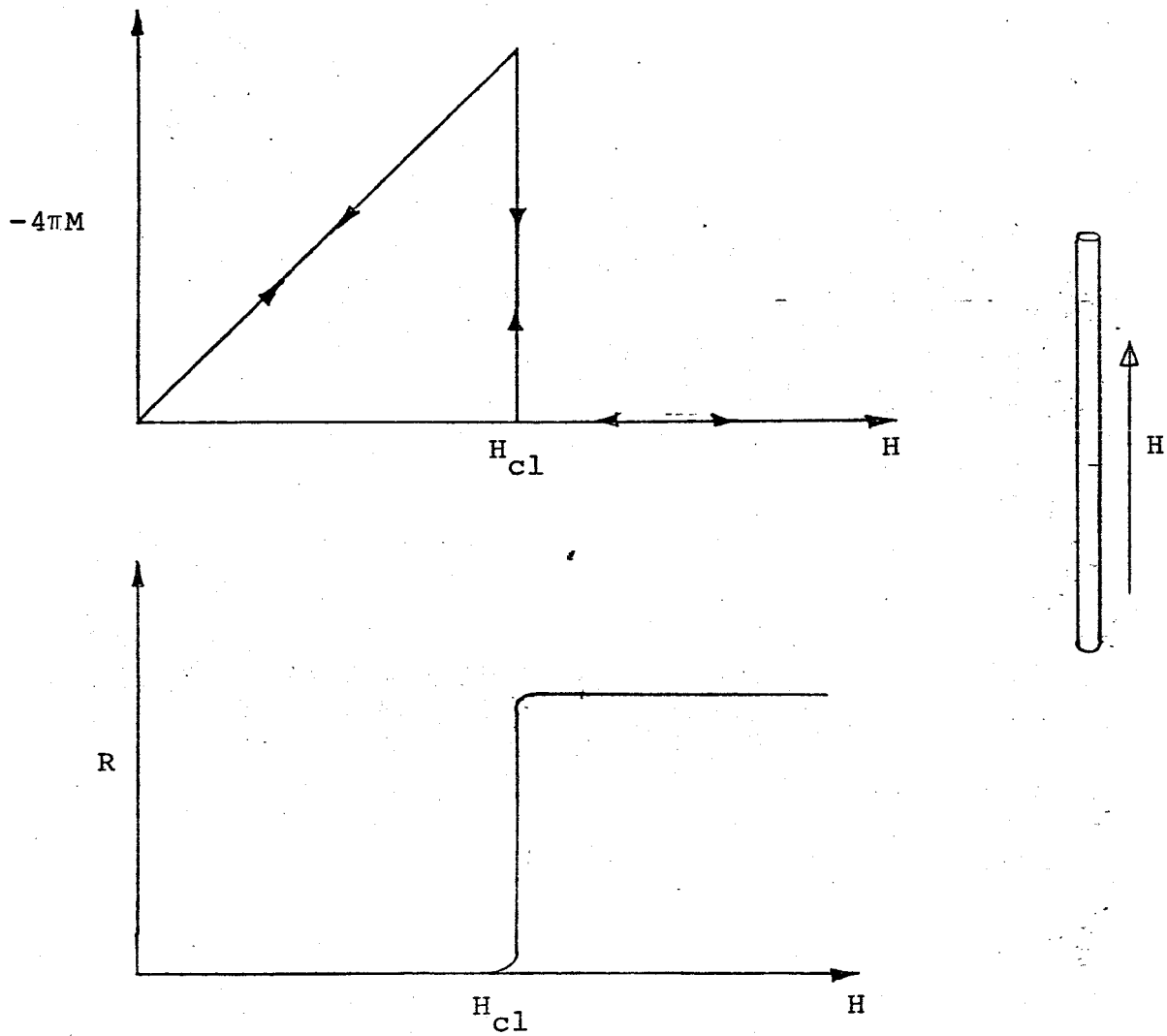


Figure 2. Magnetization and Resistance vs. External Field for a Type I Superconductor (4)

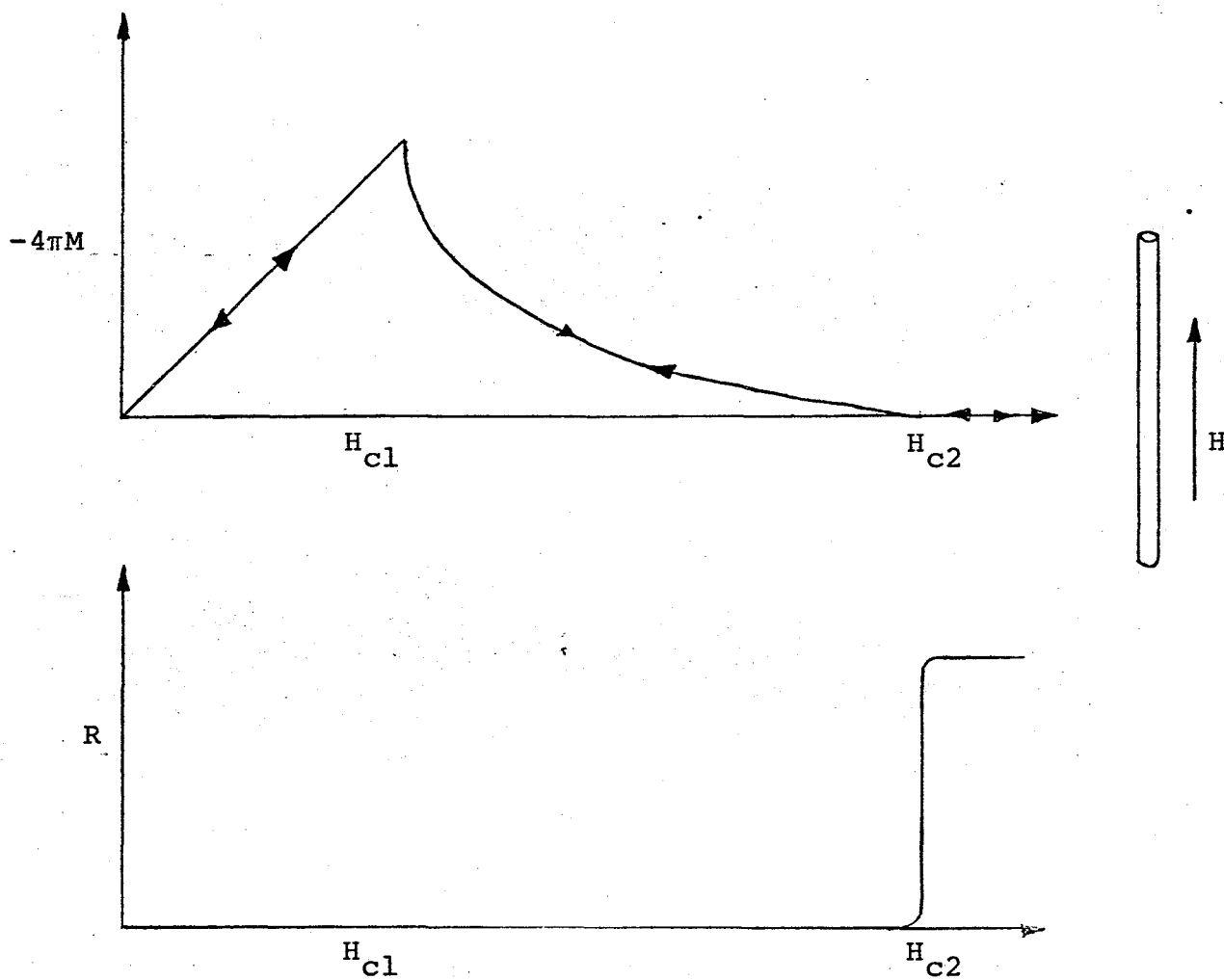


Figure 3. Magnetization and Resistance vs. External Field for a Type II Superconductor (4)

alloy, NbZr Niobium-Zirconium alloy and Nb-Sn Niobium-Tin compound.

Figure 4 shows the type of relation between maximum current density (J_c) and applied magnetic field that a Type II superconductor can tolerate without transition to the normal state.

The J_c vs. B relation is approximated in two regions: a) for small perturbations, in the mid-range of the curve, the simple London approximation that J_c is independent of B is valid; b) for lower fields the Kim relation is used:

$$J_c = \frac{J_0 + B_0}{B + B_0}$$

J_0 and B_0 are constants which depend on the flux pinning strength of material and self-field of conductor.

2.3 Penetration Depth and Hysteresis Losses

For a changing field perpendicular to a cylindrical wire penetration depth (2) is

$$\lambda = \frac{2\pi B}{\mu_0 J_c}$$

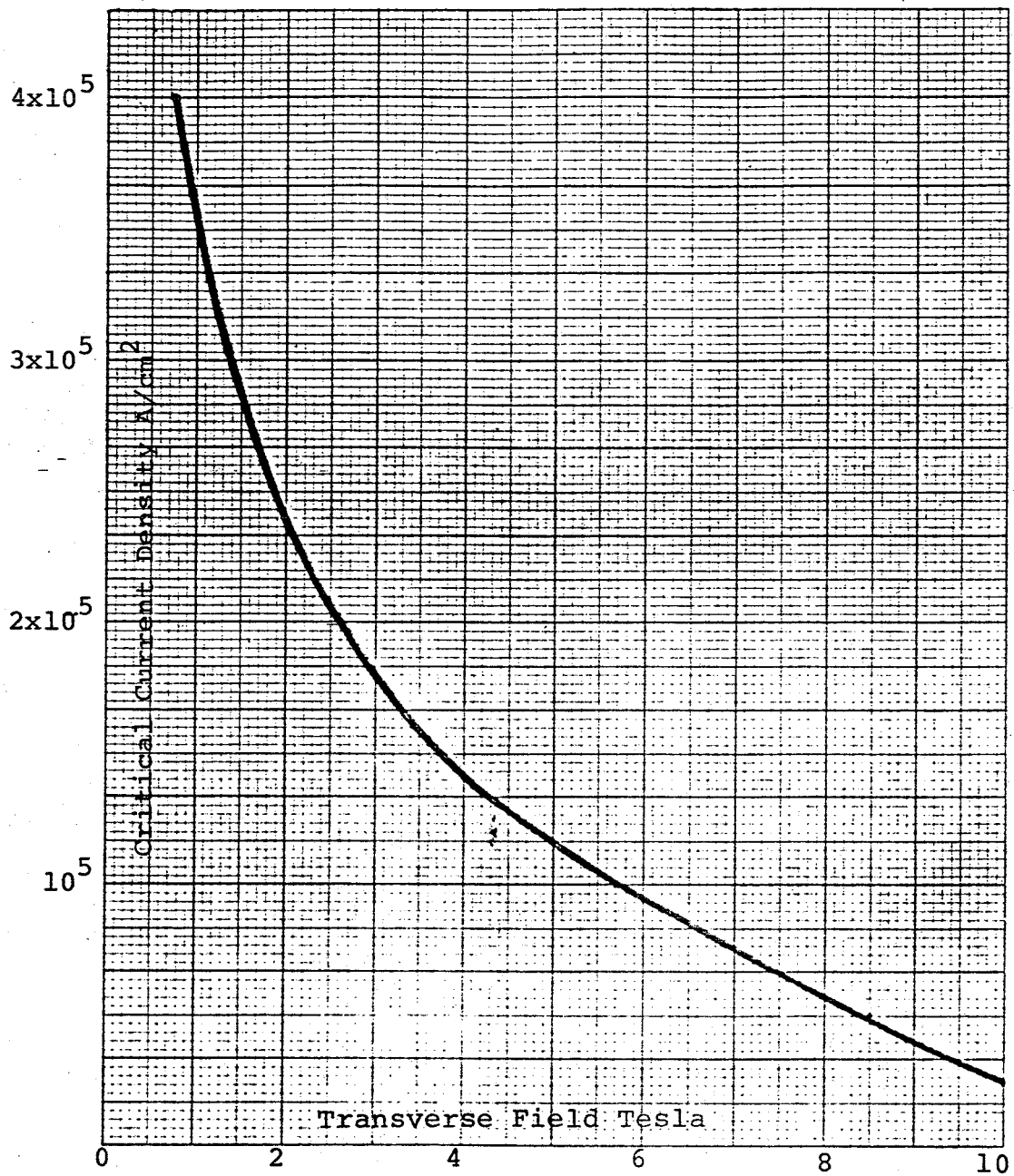


Figure 4. Typical Current Density Relations vs. Transverse Magnetic Field for a Type II Superconductor Alloy (1)

ORIGINAL PAGE IS
OF POOR QUALITY

The necessary field change to fully penetrate the conductor in the London approximation is

$$B_p = \frac{\mu_0 J_c d}{r} \quad (1)$$

For a varying field as (1) shows, since the current density is limited, the field that can be shielded is also limited. At fields higher than B_p , the field has reached to the center of conductor and any change in external field will appear instantaneously in the conductor. However, the magnitude of the interior field will lag behind an increasing field or a decreasing external field. This causes hysteresis losses for Type II superconductor in varying fields.

Chapter III

DESIGN

3.1 The Magnetic Suspension and Balance System

The present M.S.B. (NASA-MIT Balance) at the M.I.T. Aerophysics Laboratory uses three main groups of copper-wired coils, cooled with water, with iron poles for controlling and producing forces and moments in different directions (3). The three groups of coils are as follows:

- a) Helmholtz-coil system (controls \bar{B}_x, \bar{B}_{xx})
- b) Saddle-coil system (controls \bar{B}_y, \bar{B}_z)
- c) Side and lift force system (controls $\bar{B}_{zx}, \bar{B}_{yx}$)

Figure 5 shows the arrangement of these coils. Besides these, there is an Electromagnetic Position Sensor Coil System, which measures the position of the model for controlling it.

Since the main sources of power consumption are coils in groups (a) and (c) and the iron poles of group (c), (Figure 6), limit the field and makes scaling unreliable, it was decided to design coils (a) and (c) using superconductors and no iron.

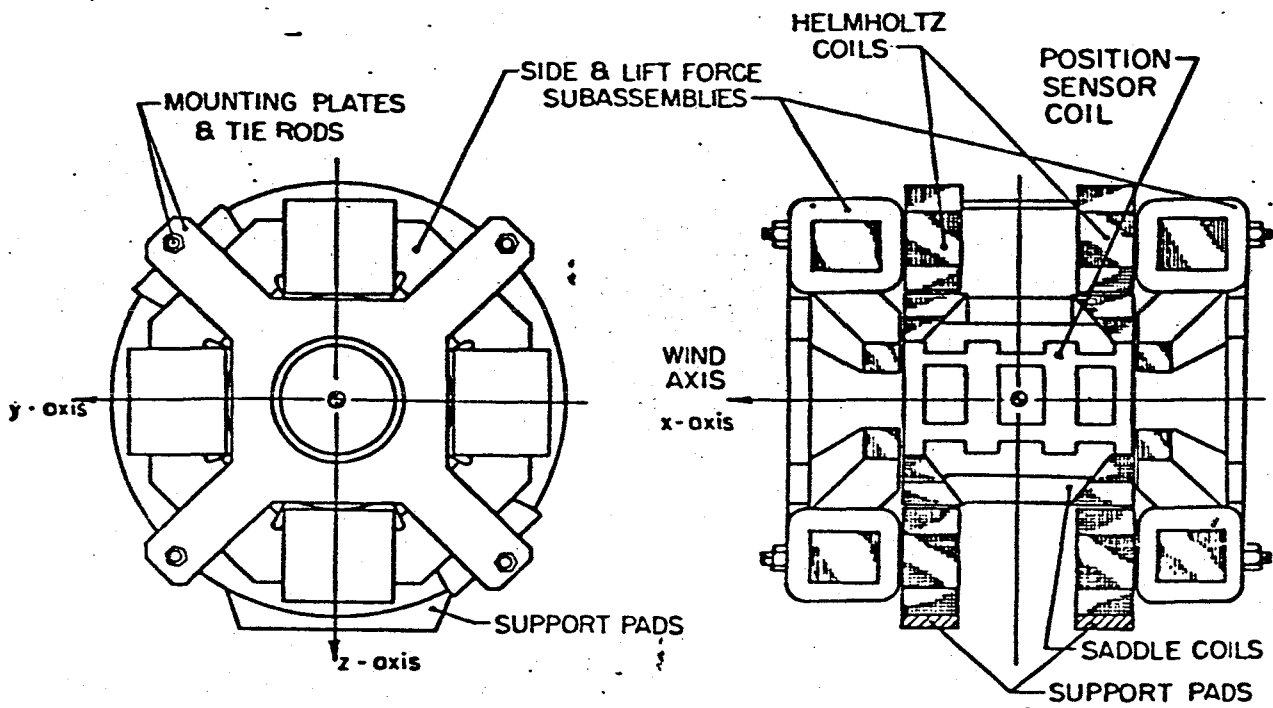


Figure 5. Assembly of Magnet System (3)

ORIGINAL PAGE IS
OF POOR QUALITY

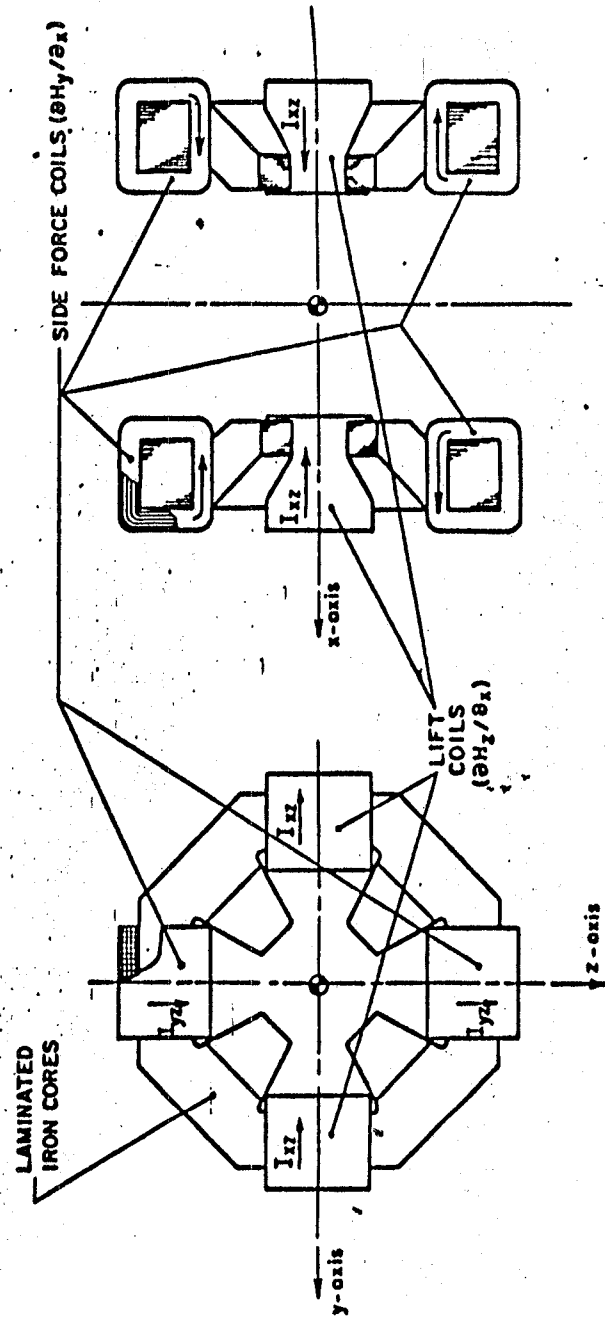


Figure 6. Side and Lift Coil Assembly (3)

ORIGINAL PAGE IS
OF POOR QUALITY

The main constraints for such a design are as follows:

(a) The whole superconducting coils should be in one or two warm bore dewars.

(b) Enough light passage to watch the model or use measuring optic devices such as LDA should be provided.

(c) The saddle coil system and position sensor coils should remain in their position.

The remaining space is shown in Figure 7.

3.2 Computer Program

The computer program (TABLE) (5,12,13) tabulates the magnetic field components due to a series of straight line current elements or a series of circular line current elements. In the straight line current element mode it is limited to the shapes which could be approximated by straight lines. Figure 8 shows a sample winding that can be handled by TABLE.

The number of turns in computer program is controlled by M and N (number of layers and turns per layer in winding cross-section). The effect of changing these parameters and convergence of computer results are discussed in Appendix 1.

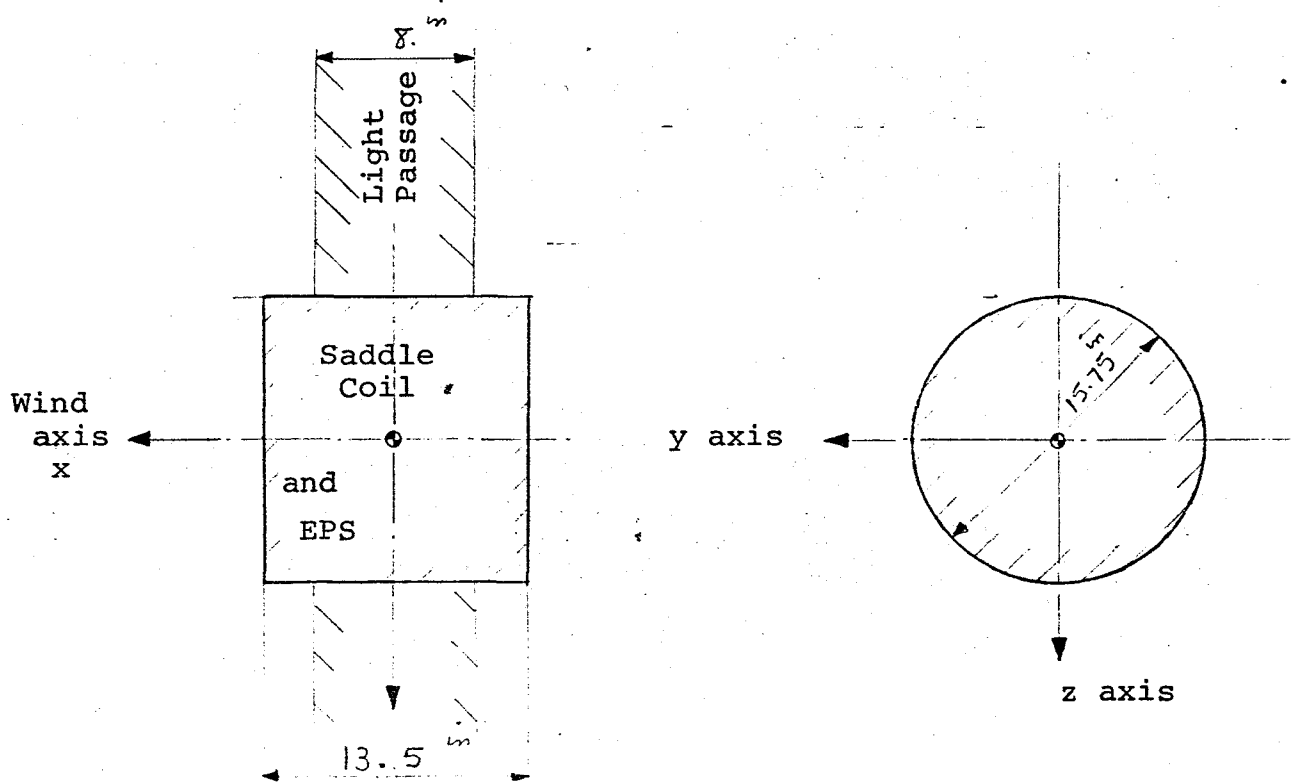


Figure 7. Free Space for Design (Unhatched)

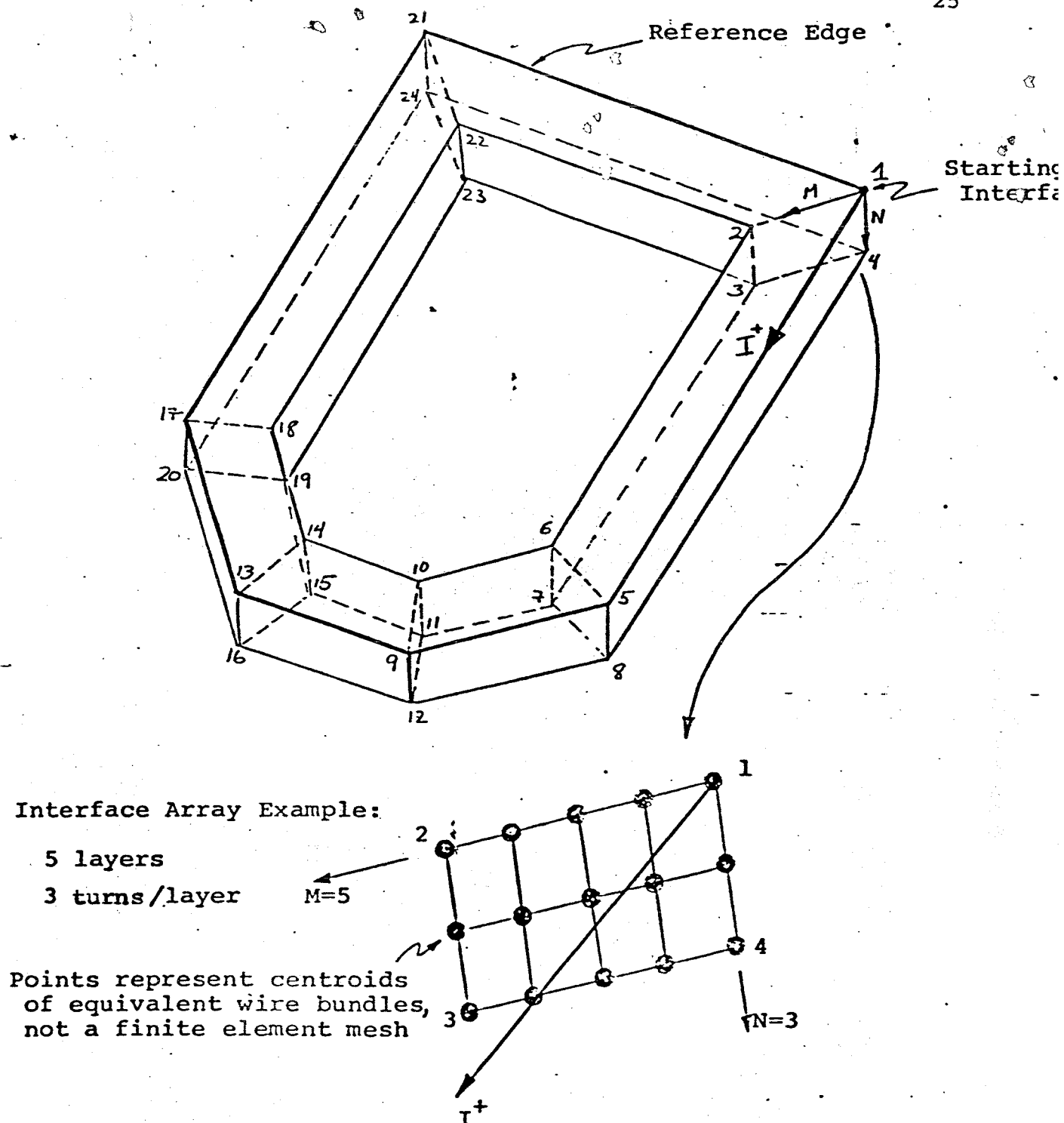


Figure 8. Sample Coil Geometry Specification

3.3 Testing Computer Program

A model coil similar to the designed lift coil system (Figure 9) was made to measure the transverse field component on wind axis and compare with TABLE predictions for the same coil system (14).

Figure 10 shows the results of TABLE together with measured results. The computer program overestimates about 10 percent, which could be explained by noticing the procedure in which TABLE locates the wires in the winding volume. The cross-section of the model coil was not rectangular, so the results might be improved to some extent for a rectangular winding cross-section. The second important source of computer program error is that TABLE approximates the curves at winding corners with the intersection of two straight lines.

3.4 Finding the Best Configuration

The present side and lift coil system with iron poles (Figure 6) has a measured performance of:

$$\bar{B}_{zx} = 1.4 I_{zx}$$

Taking $I_{zx} = 385A$, the gradient should be 540 gauss/in.

This is the basic requirement chosen for each different configuration of air core superconducting side and lift coils.

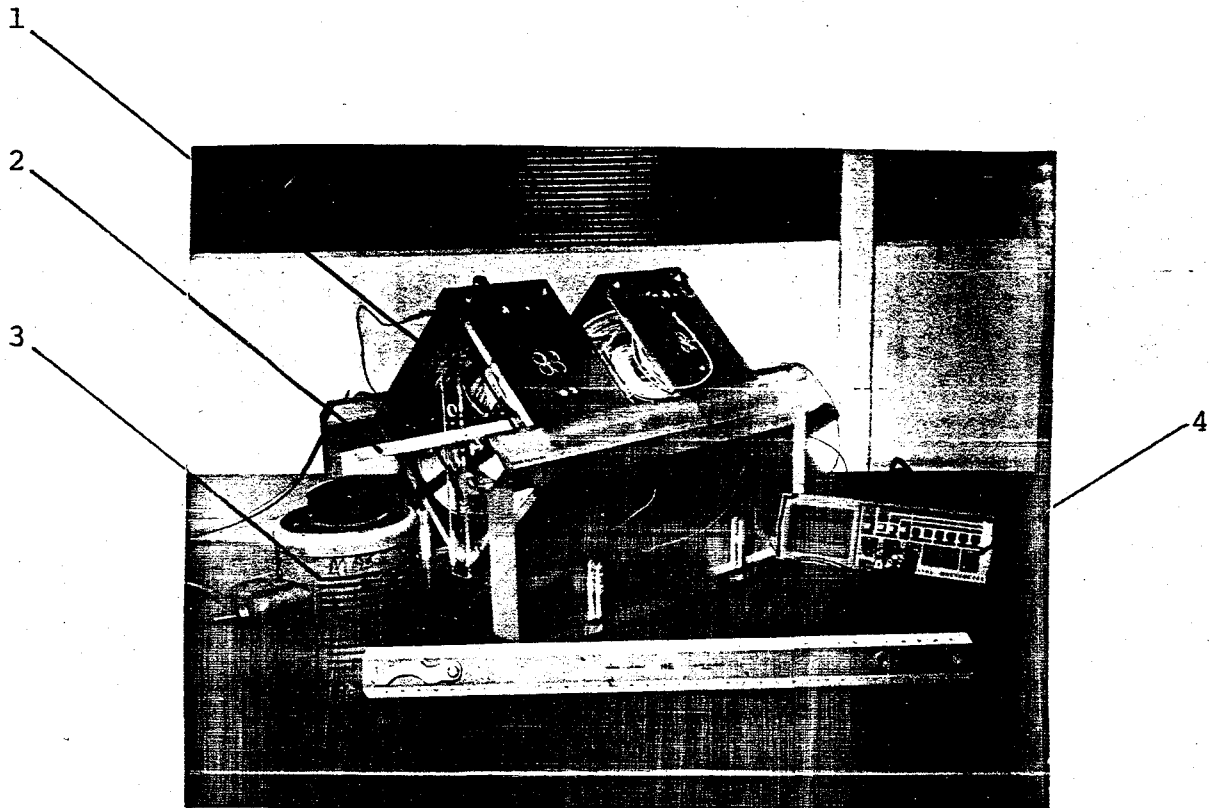


Figure 9. Model Coil for Testing TABLE

- | | |
|------------------------|--------------------------|
| 1 Model coil | 3 A.C. transformer |
| 2 Pick-up coil support | 4 Pick-up coil voltmeter |

ORIGINAL PAGE IS
OF POOR QUALITY

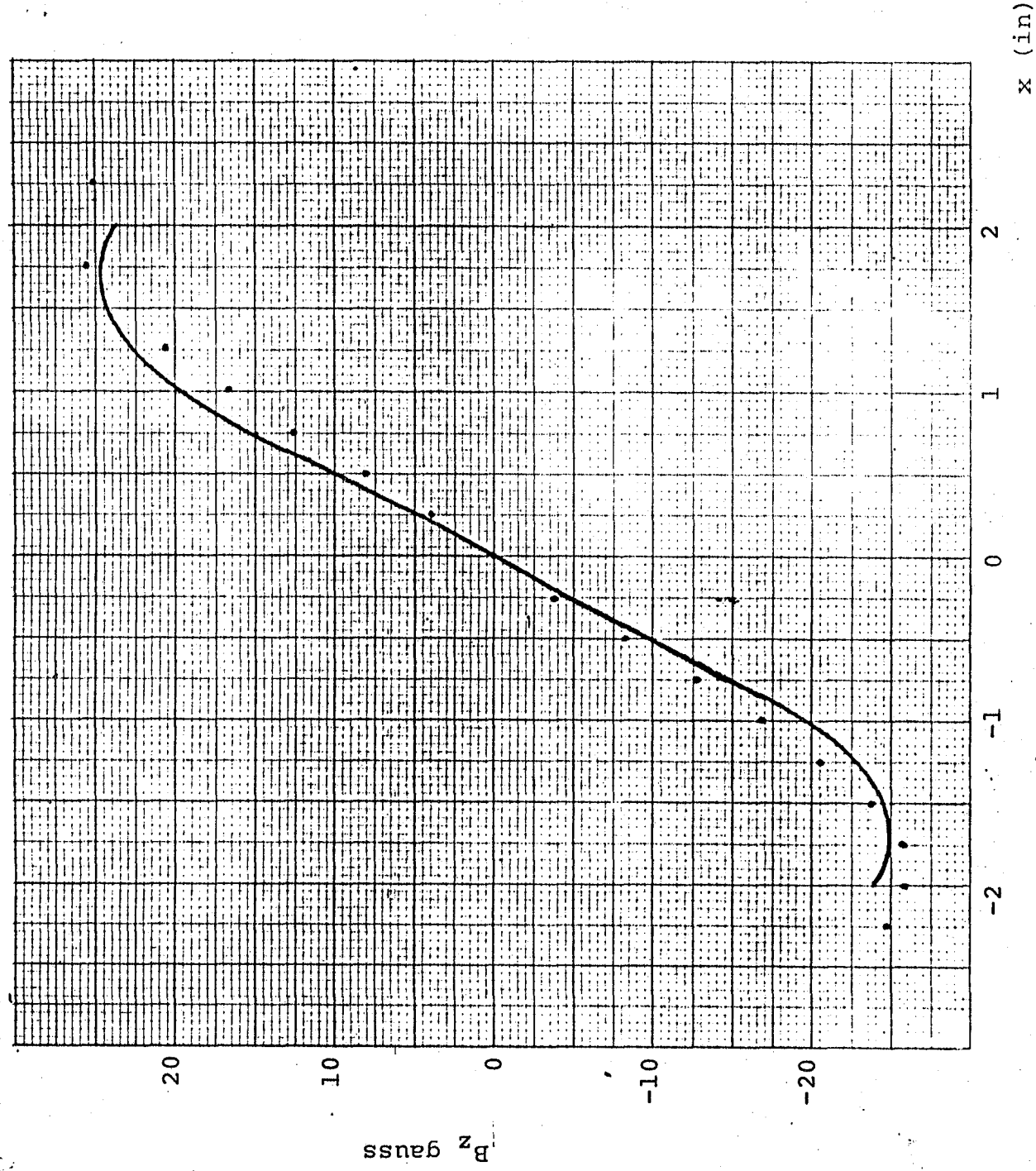


Figure 10. Transverse Field Component
vs. Axial Distance

Computer Results

Model Measurements

As a first step a model coil with the same core form as the iron poles was tested as Model I (Figure 11). Since the performance was not satisfactory and winding was difficult, the winding plane is not perpendicular to the core form axis so it is possible that the wires slip; Model II with the same core shape but with the winding plane perpendicular to the core axis was tried. Figure 12 shows the direction of wires and the different angle of core for which computation was done. The disadvantage with this model is that due to its acute angle of winding with the axis plane, it takes a lot of space and leaves the unoccupied space unusable.

Figure 13 shows Model III. This model came about as an approximation to Model II and since it uses all available space, it is a better choice in most cases.

Choosing a configuration depends on the magnitude of gradient which is needed. For a low transverse field gradient ($\bar{B}_{zx} < 200$ gauss/in). Model I and Model II are comparable to Model III but at field gradients as high as ($\bar{B}_{zx} = 500$ gauss/in). Model III is considerably superior. For producing

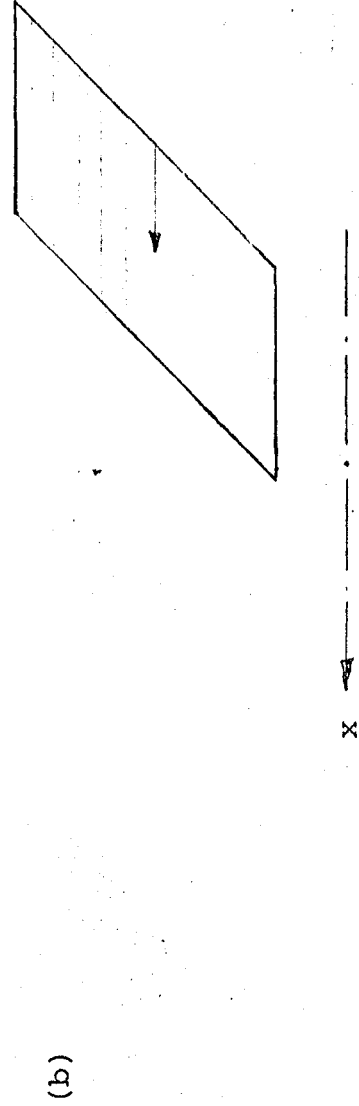
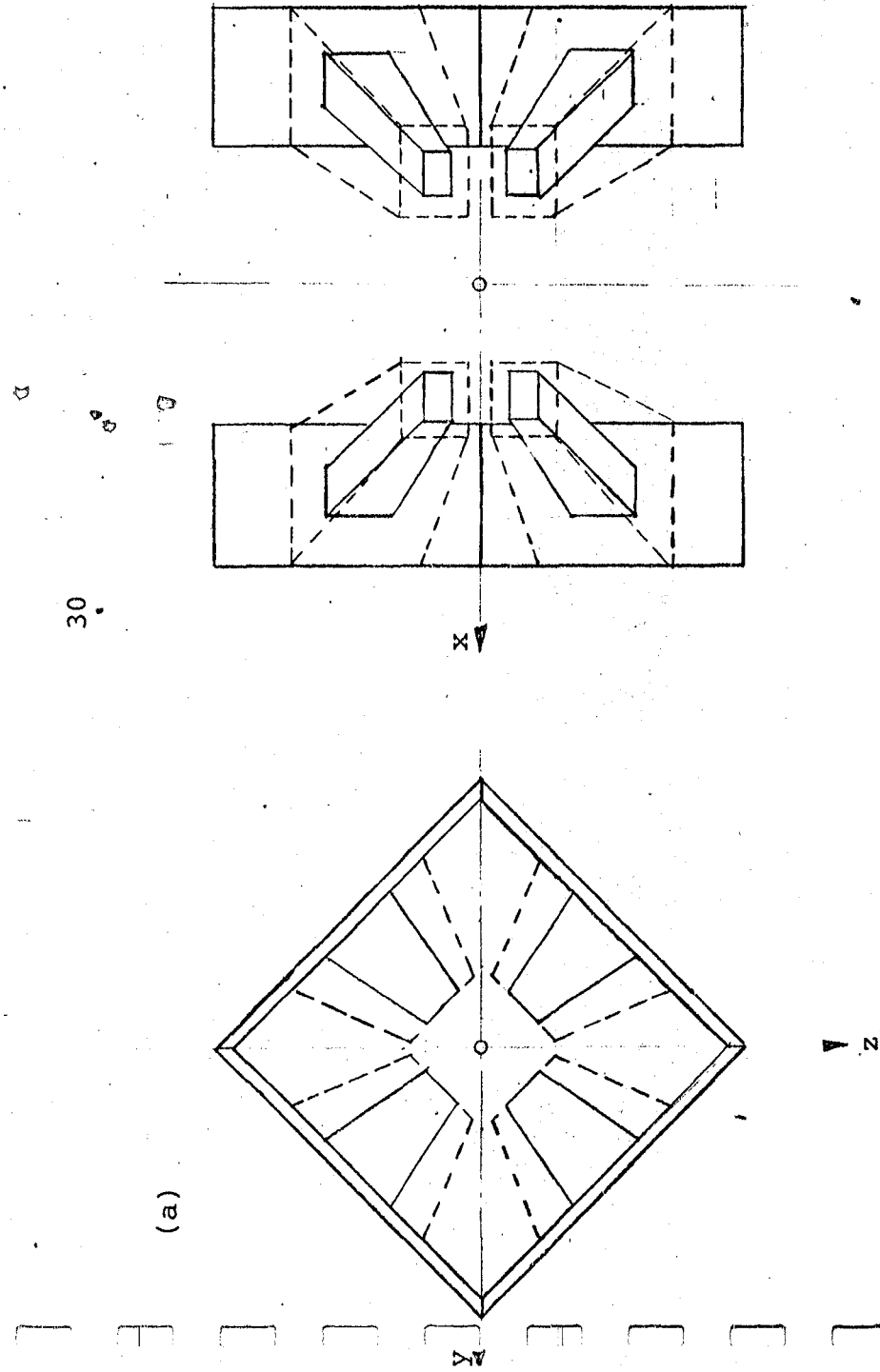
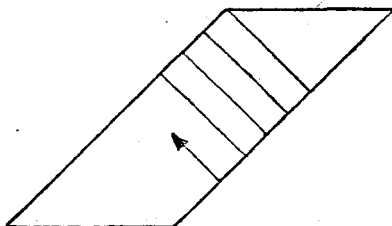


Figure 11. a) Model I
b) Direction of Wires

31



x

(a)

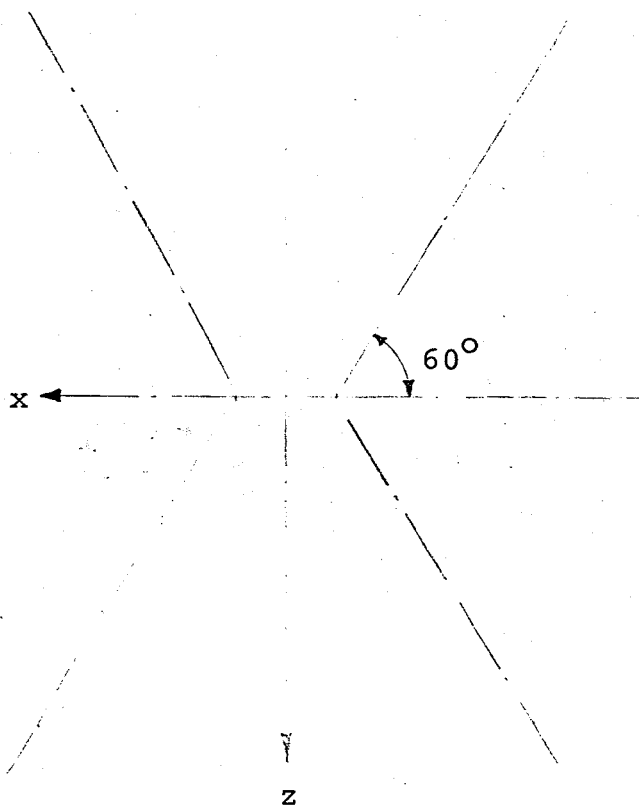
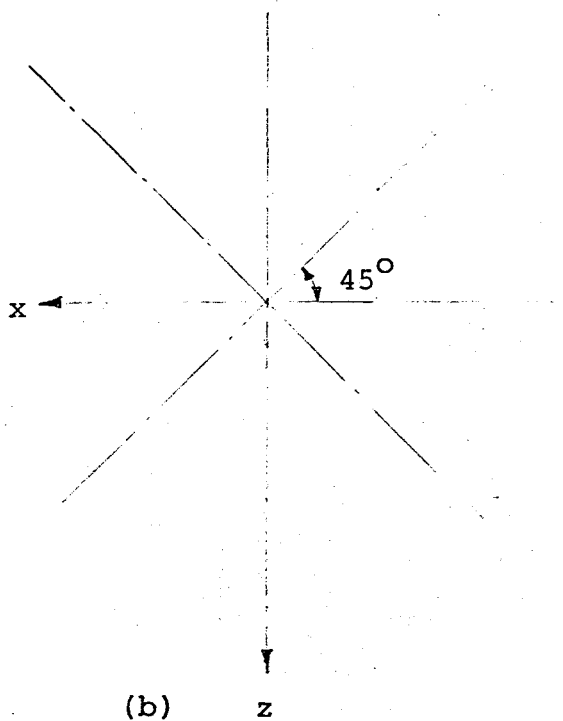
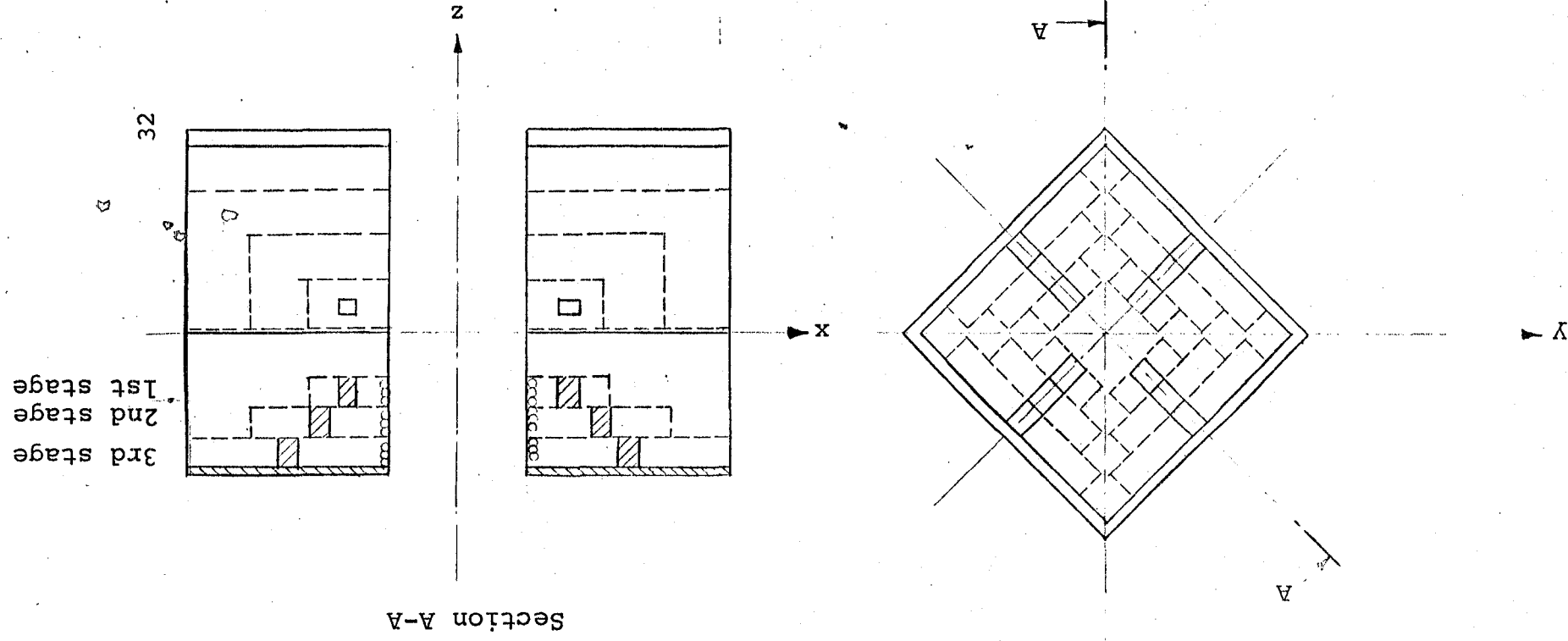


Figure 12. Model II a) Direction of Wires
b) Different Core Axis

ORIGINAL PAGE IS
OF POOR QUALITY

Figure 13. Model III



500 gauss/in gradient, Model II at 60° core axis angle should have 5000 turns in each of 8 coils whereas Model III with three-stage optimized coils needs 3900 turns in each of 8 locations. This should be clear since for extending Model III upper stages would be closer to the center than upper stages of Model II.

Model III can be optimized easily if the effect of each stage is studied separately. Such an investigation shows that at a definite radial position the highest gradient may be obtained from one stage. Table I shows the $\bar{B}_{zx}/(\text{ampere turn})$ for each stage in Figure 13 and a fourth stage that might be added. Stage one was discarded after such a study because it is far from the optimum radius and its contribution to total gradient is negligible. Table I shows that the optimum radius is about the place where stage 3 is. It seems the optimum radius depends on axial distance of two sets besides the geometrical parameters of winding.

It is noticeable that due to symmetry, computation of the field of one coil of each stage is enough to compute the total field for points on the x axis (axis of symmetry). This could save a lot of CPU time.

Table I

Transverse Field Gradient of Different Stages
of the Side and Lift Coil Model

Stage	Mean Radius in	Gradient \bar{B}_{zx} gauss/ in	Ampere Turn	\bar{B}_{zx} /Ampere Turn
1	5.5	15.6	18x24x260*	1.39×10^{-4}
2	8.5	102.	36x24x260*	4.54×10^{-4}
3	11.5	190.6	54x24x260*	5.66×10^{-4}
4	14.5	189.88	72x24x260*	4.23×10^{-4}

* 260A cable current is assumed for design purposes.

18x24, 36x24, etc. are the each lift coil number of turn;
i.e. half the total available number of turns. Refer to
Appendix 2 for more information.

Comparison of results for the three models shows that Model III is the most advantageous since

a) It can produce the desired field gradient $\bar{B}_{zx} = 540$ gauss/in with the least volume of space and superconductor.

b) It could be extended for higher field gradients.

c) Construction of such a coil system would be less troublesome since there is no force in windings due to unusual wire direction.

Figure 14 shows the B_z component of magnetic field for points on x axis. The B_{zx} gradient at the center is 586.8 gauss/in with gradient uniformity 12% over a sphere of radius 3 in. The average gradient is $\bar{B}_{zx} = 619$ gauss/in over a distance from $x = -3$ to $x = 3$.

3.5 Magnetizing and Drag Coils

After dimensions of side and lift coil system were found, the magnetizing and drag coil system (Helmholtz coils) could be designed according to the following considerations:

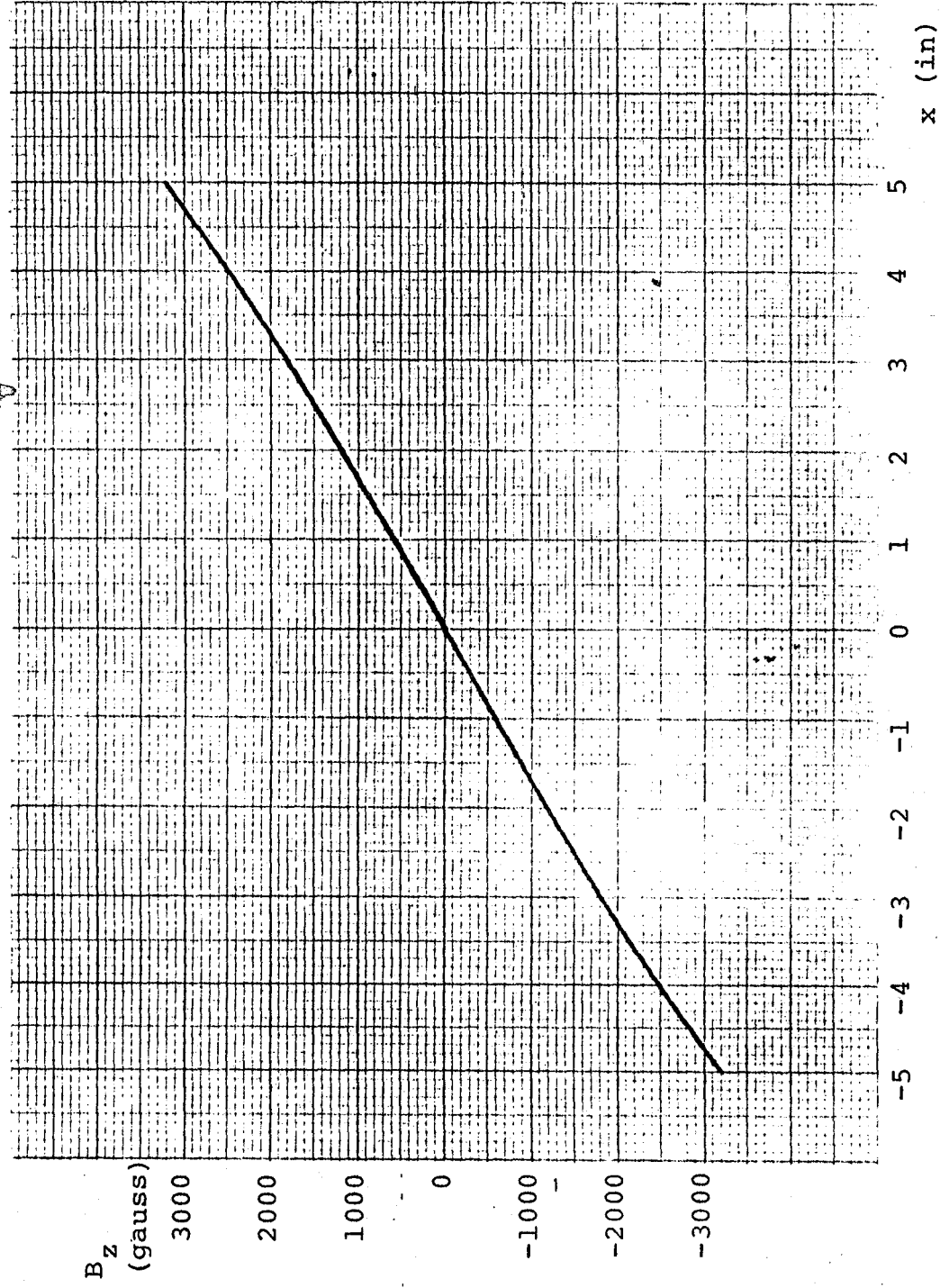


Figure 14. B_z vs. Axial Distance x
for Side and Lift Coil

ORIGINAL PAGE IS
OF POOR QUALITY

a) Magnetizing and drag coils should produce $B_x = 7700$ gauss and $\bar{B}_{xx} = 655$ gauss/in according to the measured performance:

$$B_x = 20 I_x$$

$$\bar{B}_{xx} = 1.7 I_{xx}$$

for present M.S.B. and $I_x = I_{xx} = 385A$

b) Drag coils should be inside magnetizing for less impedance, so the inner diameter is the outer diameter allowed by side and lift coil system.

c) Magnetizing and drag coils should be optimized for the least volume or least inside field, since several dimensions are possible trade-off between least volume and least field design should be effected regarding losses against superconducting material expenses. This part should be done after loss computation. Note that A.C. losses were not computed as a part of this study.

Computations for these coils were carried out by using a circular current element program (2).

Figures 15 and 16 show B_x vs. axial distance for magnetizing and drag coils. Magnetizing coils have a field component, $B_x = 7448$ gauss with a uniformity of .92 percent over a sphere of radius 3 in and corresponding values for the drag coils are $B_{xx} = 634.7$ gauss/in at the center with gradient uniformity 6.5 percent over a sphere of radius 3 in.

Figure 17 shows the overall designed coils with present saddle and position sensor coils. All superconducting coils were designed for 260A operation. Note that the Helmholtz coils are not separated by the theoretically ideal distance. This is also true of the NASA prototype Helmholtz coils, which are approximately positioned.

3.6 Magnetic Field inside Coils and the Conductor Size

For finding proper diameter of conductor using Figure 4, one should have the magnetic field due to all coils inside windings. From these, current density should be determined to be less than J_c . TABLE was used for this purpose and the field at different wire

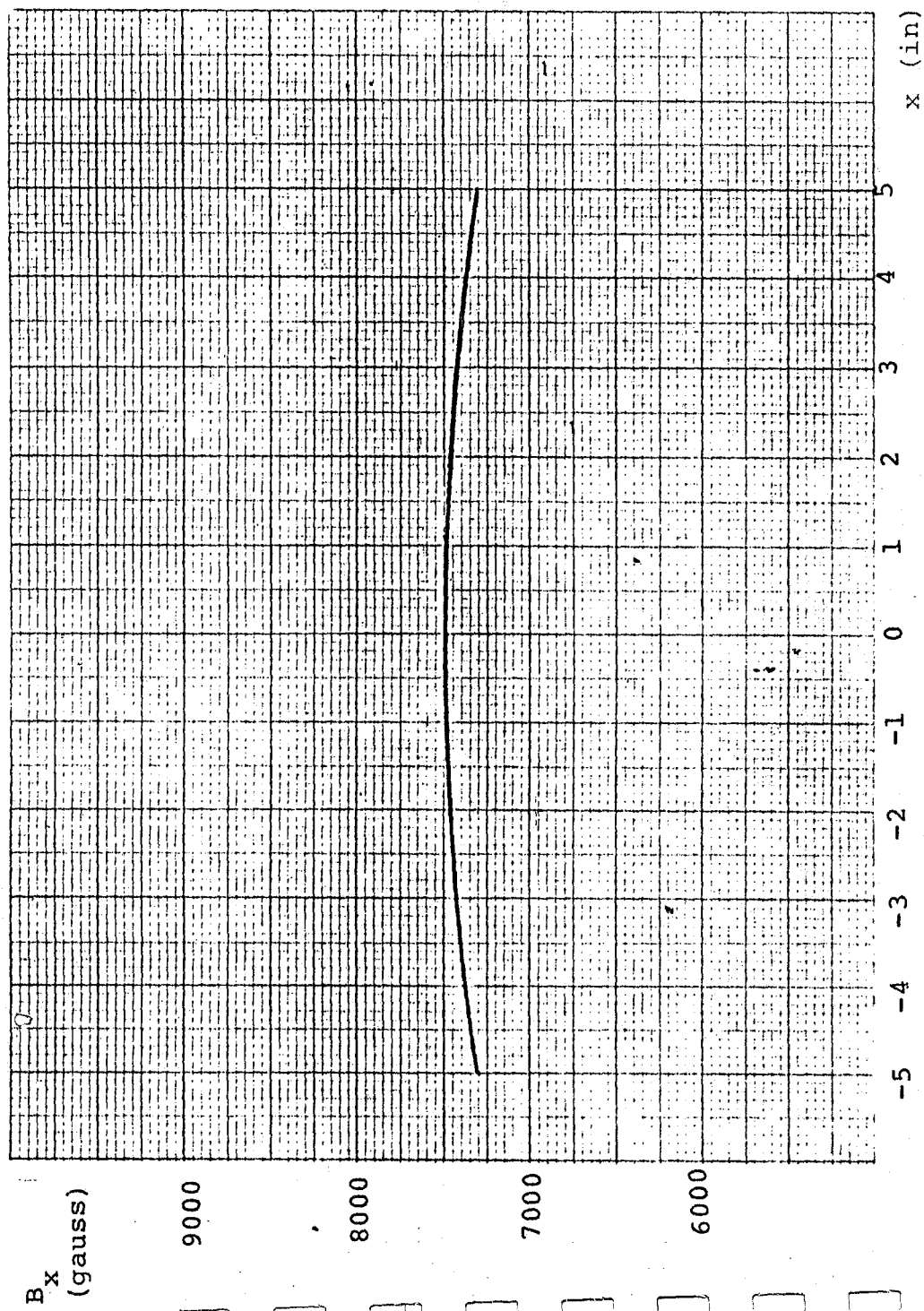


Figure 15. B_x vs. Axial Distance x
for Magnetizing Coils

ORIGINAL PAGE IS
OF POOR QUALITY

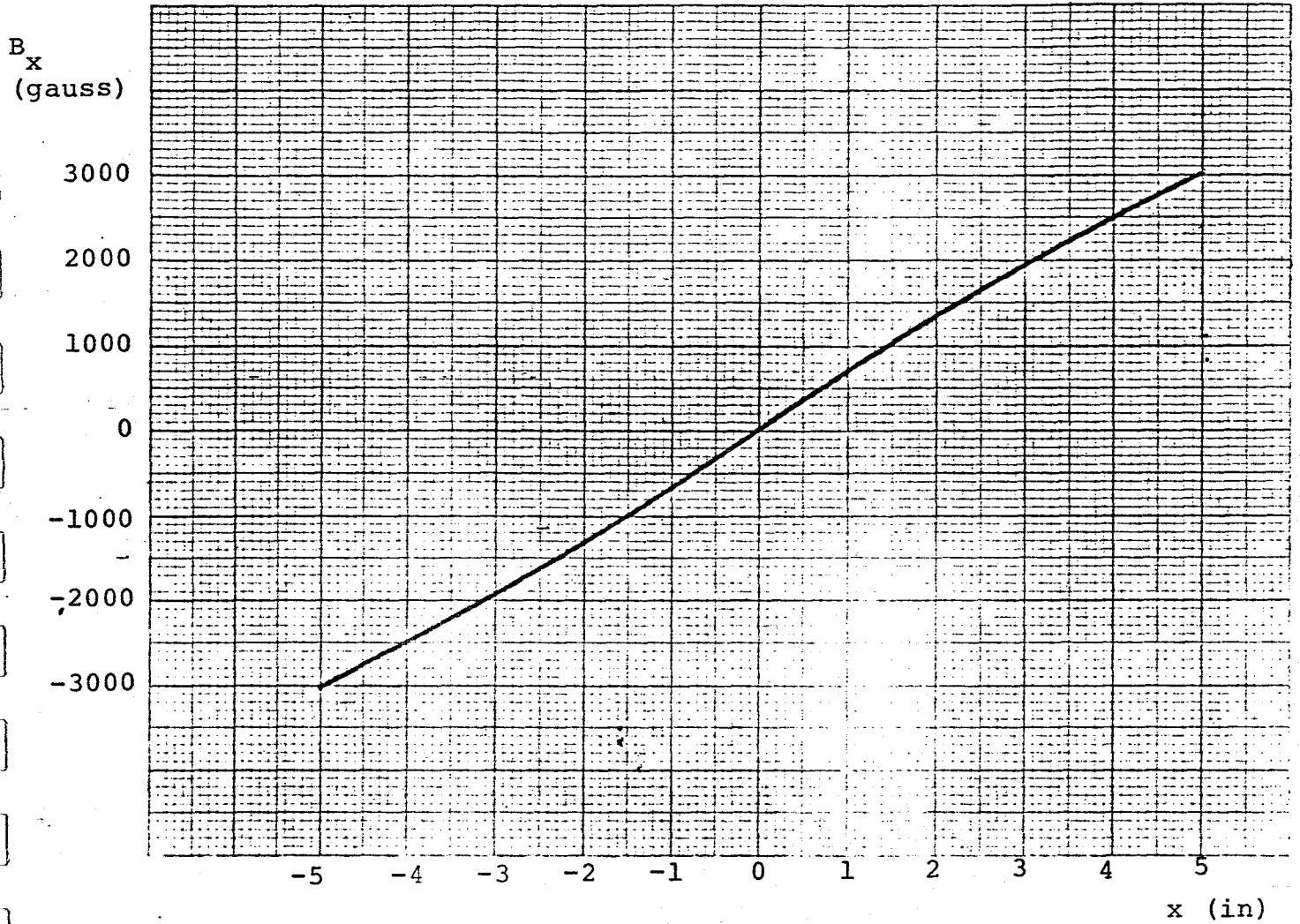


Figure 16. B_x vs. Axial Distance x
for Drag Coils

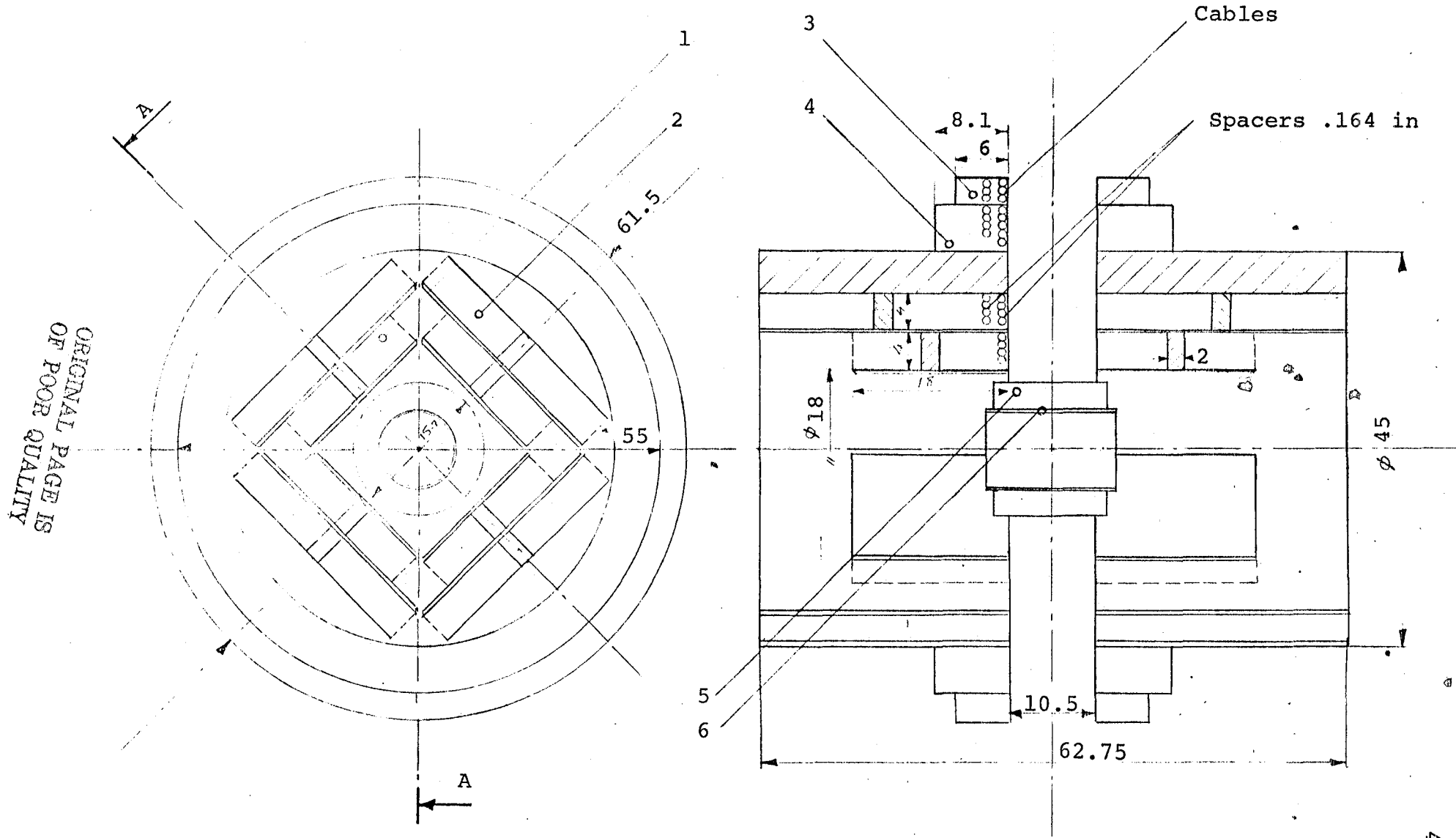


Figure 17. Assembly of Designed Coils together with Present Saddle and EPS.
Dimensions are in inches. Legends are on next page.

41a

Figure 17 Legends

<u>Reference Number</u>	<u>Coil Description</u>	<u>Req No.</u>	<u>Layer</u> *	<u>Turn per Layer</u> *
1	1st stage side and lift	8	36	42
2	2nd stage side and lift	8	52	42
3	Magnetizing	2	38	50
4	Drag	2	52	75
5	Saddle			
6	EPS			

* For side and lift force coils these figures are half the total of number of turns, accounting only for the lift coils.

locations was obtained to which the wire self field, which depends on conductor diameter, should be added later. For these computations maximum allowable number of turns were used for neighboring coils regarding convergence criteria in Appendix 1. Table II includes the maximum field inside each stage of side and lift coils, drag and magnetizing coils and the percentage contribution of each set of coils to the overall field. This field is the

magnitude of B ; i.e., $(B_x^2 + B_y^2 + B_z^2)^{1/2}$, which is perpendicular to the wires. The maximum field is found from a comprehensive study for each set of coils. Figures 18 through 21 show the magnitude of the magnetic field inside respective coils. Figure 20 shows the field distribution in two drag coils, since prediction of the worst one is difficult. In each computation absolute value of each field component due to side and lift coils were added to the absolute value of the same component of the drag and magnetizing field.

One can define the appropriate conductor size either by maximum field in the worst coil, or by the

Table II

Maximum Magnetic Field Inside Coils
with Percentage of Contribution of each Set

Coil Description	% Self Field	% of Cont. of S&L 1st	% of Cont. of S&L 2nd	% Magnetizing	% Drag	Max Field Tesla
S & L Coil 1st stage	27.5	2.6	31.2	11.8	26.8	3.71
S & L Coil 2nd stage	35.1	23.6	5.3	11.1	24.9	3.71
Drag Coil	41.	1.	2.	51.1	4.1	3.56
Magnetizing Coil	34.	8.	15.4	4.9	37.7	2.81

Ellipses represent field
magnitude between:



3.71 - 3.34

3.34 - 2.97

2.97 - 2.58

2.58 - 2.21

less than 2.21

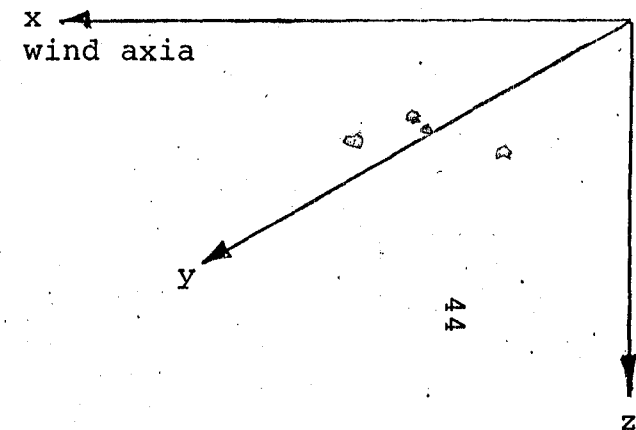
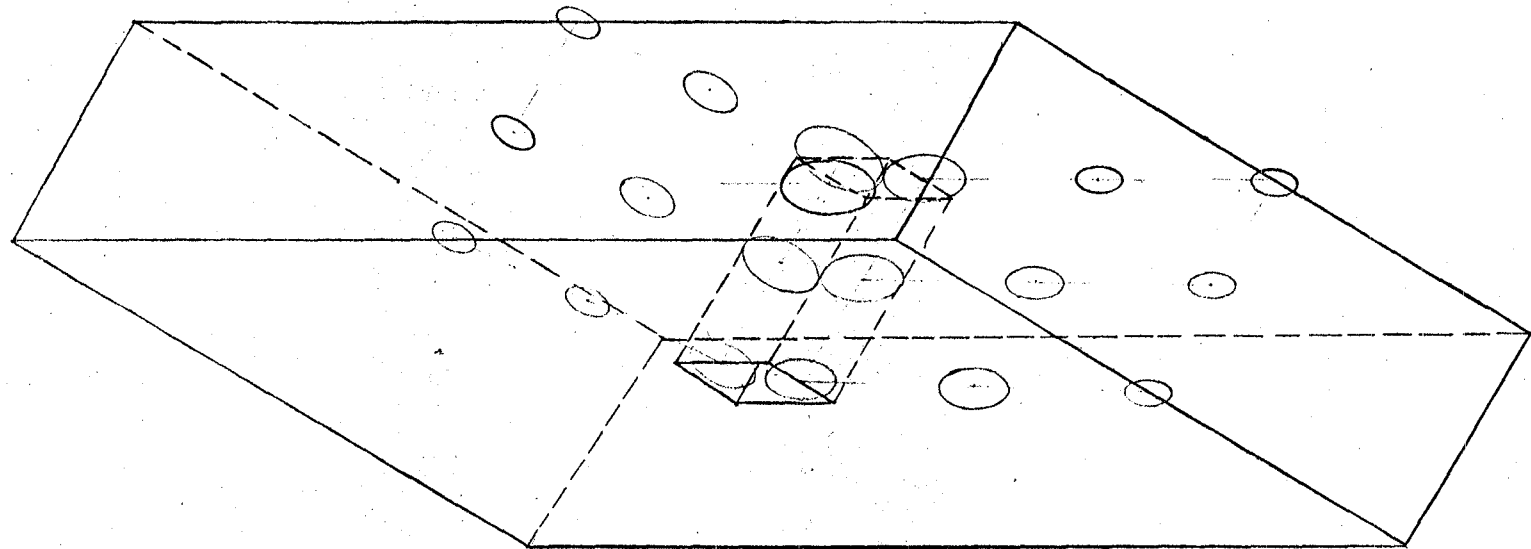
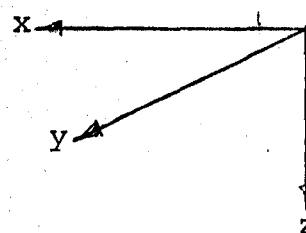
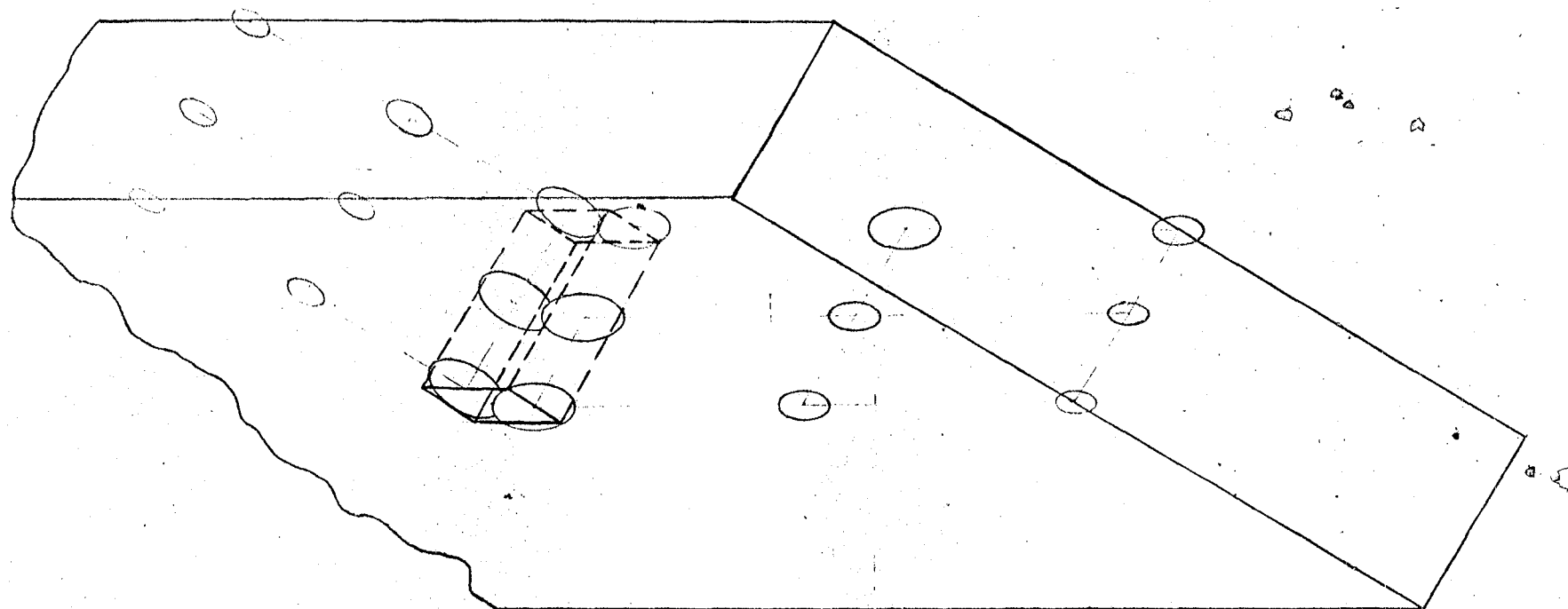


Figure 18. Field Magnitude in
Side and Lift Coil, 1st stage

ORIGINAL PAGE IS
OF POOR QUALITY



Field magnitude between:
Tesla






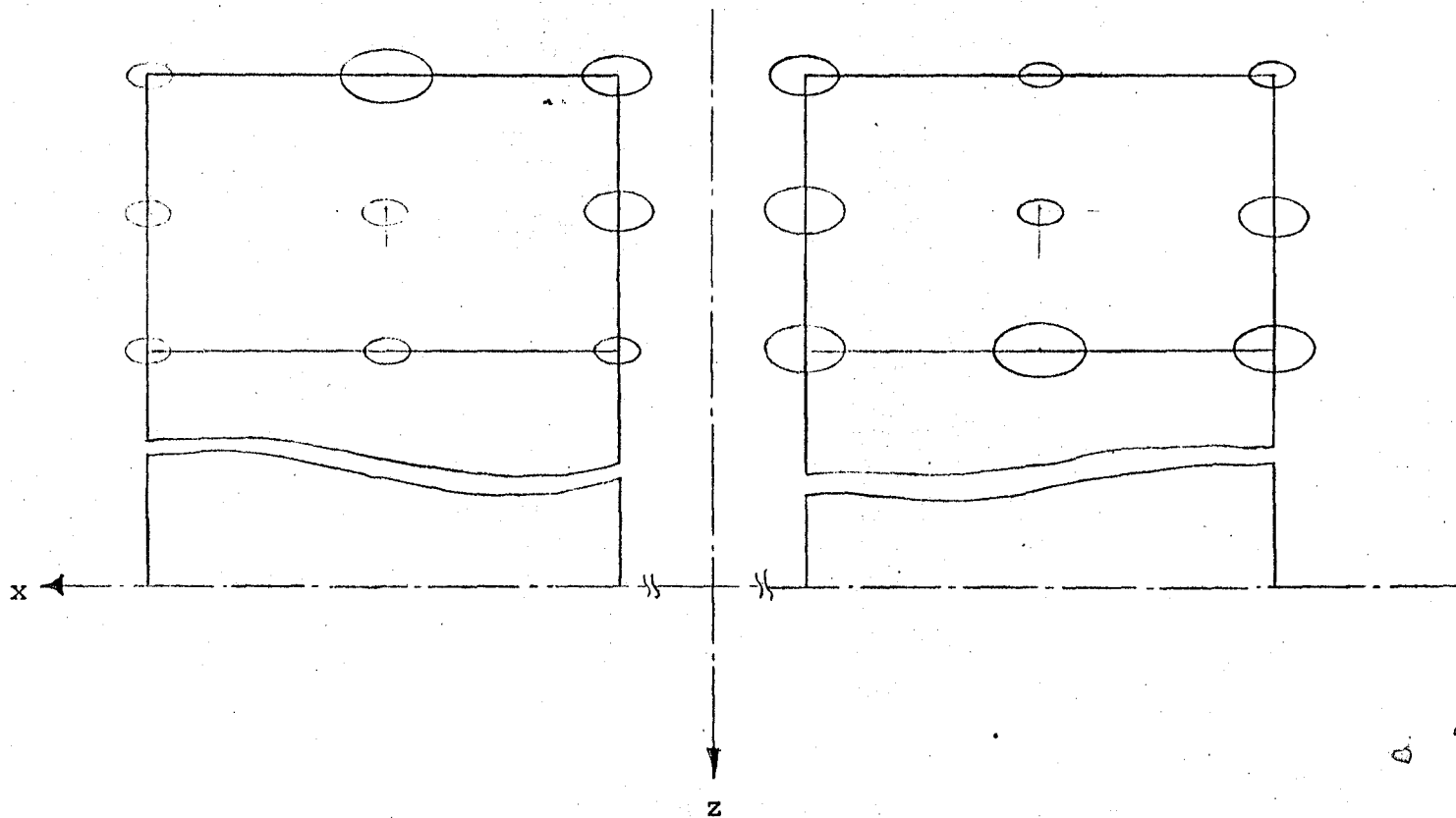
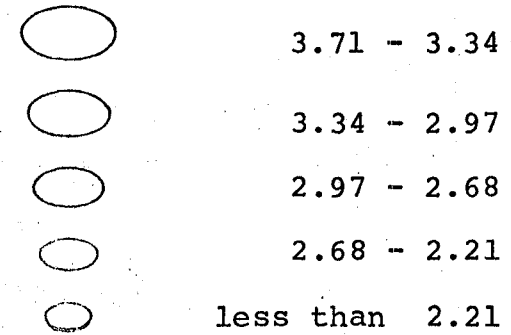
	3.71 - 3.34
	3.34 - 2.97
	2.97 - 2.58
	2.58 - 2.21
	less than 2.21

Figure 19. Field Magnitude in
Side and Lift Coil, 2nd Stage

Field magnitude between:
Tesla

Figure 20. Field Magnitude
in Drag Coils



47

Field magnitude between:
Tesla



2.81 - 2.55



2.55 - 2.29



2.29 - 2.03



2.03 - 1.77



less than 1.77

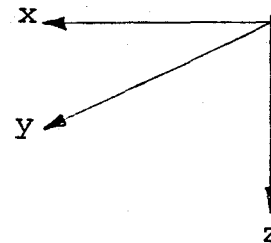
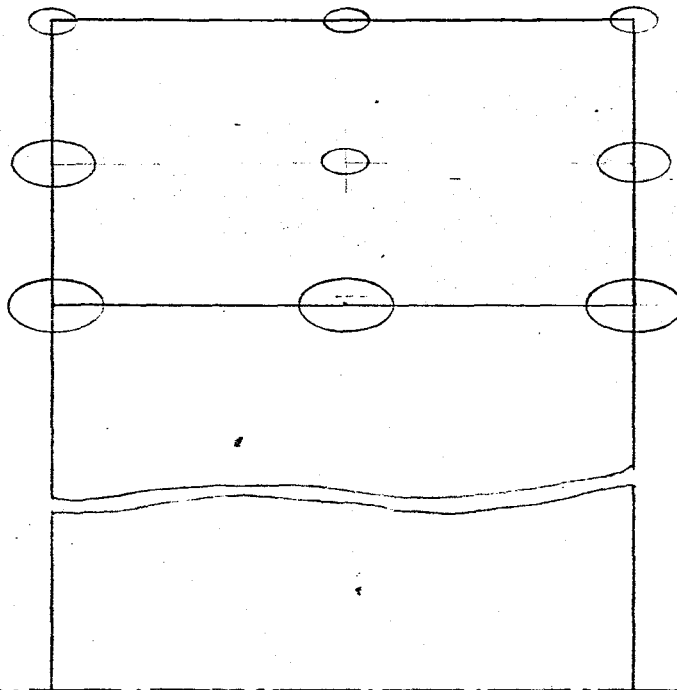


Figure 21. Field Magnitude in
Magnetizing Coil

maximum field in each coil locally. This procedure could be repeated for each single coil; i.e., dividing each coil into several parts and defining the proper conductor size for each segment based on maximum field in that segment. The second method would be advantageous in reducing superconductor volume but would require the purchase of more types of cable.

One can check the initial assumed cable size on which the field calculations were based by noticing that for every cable size trial, the current density in superconducting part of the cable should be less than the critical current density obtained from a J_c vs. B relation, such as one in Figure 4. Checking this condition leads to a new conductor size and new coil dimensions. Therefore, field calculation must be repeated until $J < J_c$ condition is satisfied. It is worth noticing that the field does not change with cable size a great deal if one keeps the number of turns constant. This may cut down the number of trial and error cycles.

After such an attempt for the proposed configuration, the proper cable dimensions are presented in Table III. The computed maximum fields were increased 20 percent to take into account the possible computer error and other factors.

The proposed conductor is a cable of solid NbTi core filaments, which diameter of filament is .0367 mm with copper/superconductor ratio = 1.71/1. This conductor was tested in (1) and (2) and was proved to be the best conductor solution available in market for present application.

Table III

Final Cable Dimensions
for Different Coils

Side and Lift, 1st stage					
Cable	Dia _{mm}	S _{SC} _{mm} ²	J _{A/mm} ²	Maxfield x 1.2 Tesla	J _C A/mm ²
7x6x5	1.73	.222	1170	4.52	1250
Side and Lift, 2nd stage					
7x6x5	1.73	.222	1170	4.52	1250
Drag Coil					
8x5x5	1.69	.212	1229	4.35	1338
Magnetizing Coil					
6x5x5	1.46	.159	1639	3.46	1700

IV. DISCUSSIONS

An alternative superconducting version of side force, lift, magnetizing and drag coils of the present M.S.B. was presented.

Without any iron poles the side and lift coil system requires seventeen times more ampere turns to produce the same gradient. However, this ratio could be reduced drastically by decreasing the axial distance between two parts of side and lift coils.

The presented design could be more compact if a coil form such as one used for saddle coils were used for side and lift coils and also if the drag and magnetizing coils were relocated.

Choosing conductor size upon local field (i.e., the maximum field in each segment of a coil) might reduce the required superconductor volume to some extent. By dividing the side and lift coil 1st stage into two equal inner and outer parts and choosing the appropriate conductor size for each segment (i.e., an 8x4x5 cable instead of a 7x6x5 cable for outer part), one might save above 16.7% in superconducting volume for the 1st stage coils. However, it is clear that for such a partition all coils of 1st stage should have the same field distribution. For example, this procedure

is not applicable to the drag coils since they have a much different field distribution (Figure 20). Perhaps the conductor should be selected for each of them separately.

Appendix 1

CONVERGENCE OF COMPUTER RESULTS

As pointed out earlier, computer program TABLE approximates each winding with a series of straight line current elements. It fills the winding volume with the definite number of turns. The choice of number of turns depends on the required accuracy and the available computer time. The appropriate number of turns for every different relative distance of coil and the point should be computed separately.

Figure 22 shows the results of such a computation for a coil having winding parameters (M layers and N turns per layer), as 2 by 2, 4 by 4, 8 by 8 and 16 by 16. (Refer to Figure 8 for the definition of M and N.) The vertical axis is relative error to the previous step. Figure 22 shows that for such a configuration of coil and the point a choice of 16 by 16 winding results in an error less than 2 percent. This indicates that for smaller than 16 wires per layer the correct number should be yet but that for larger numbers a less costly price value is to substitute an equivalent 16 by 16 array for this particular configuration.

ORIGINAL PAGE IS
OF POOR QUALITY

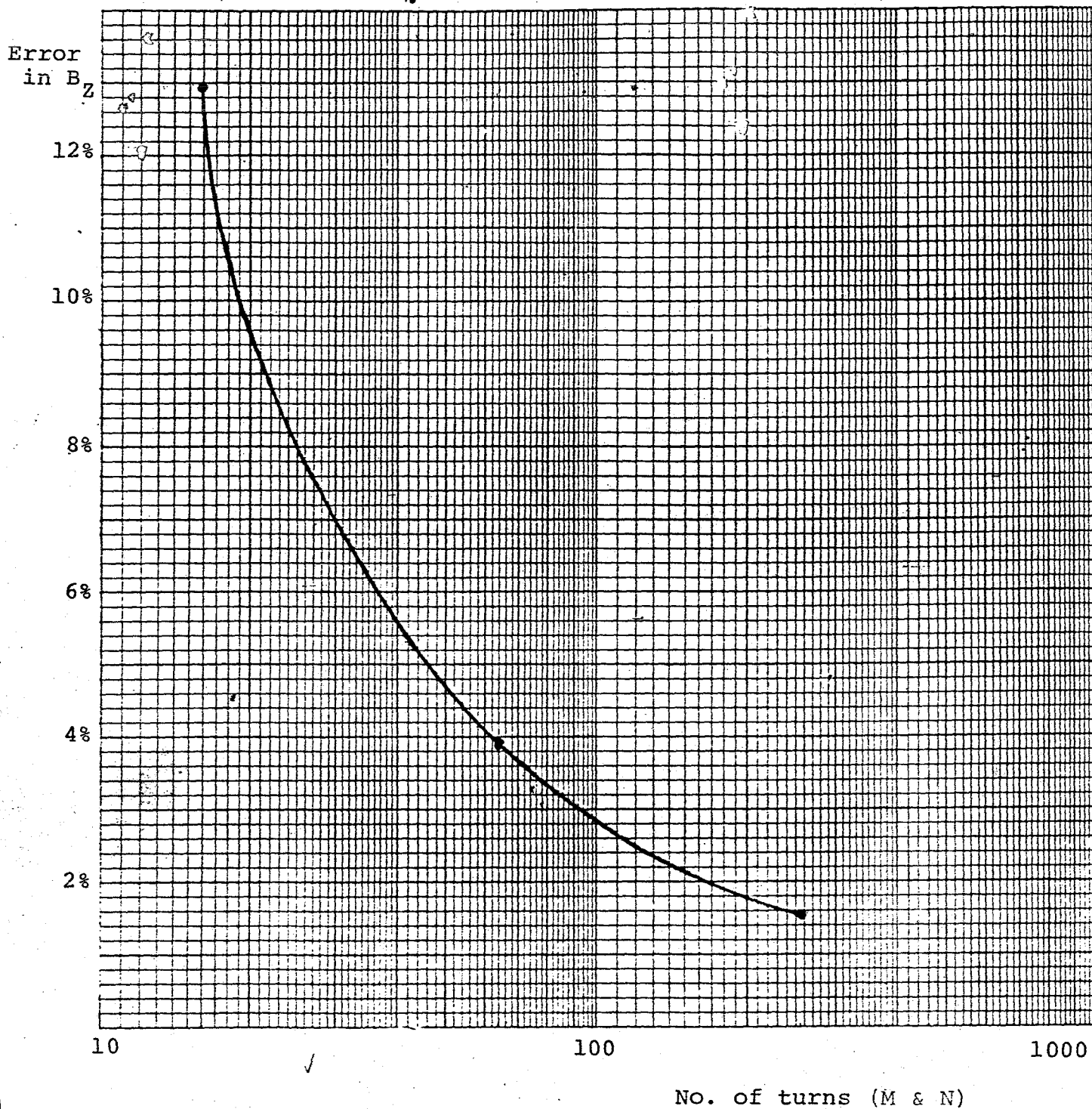


Figure 22. Convergence Characteristic
of Computer Program TABLE

ORIGINAL PAGE IS
OF POOR QUALITY

Appendix 2

COMPUTER PROGRAM TABLE
and COMPUTER RESULTS

Computer program TABLE and computer results for the designed lift force, drag and magnetizing coils are presented. The lift coils' number of turns is half the total available number of turns since the second half belongs to side force coils. Therefore, the side force field component (B_y) distribution is similar to lift force component (B_z) distribution. In practice, they are powered from a single line having the resultant current.

The complete elliptic integrals in Subroutine Circe are computed according to (10).

TABLE

Program to calculate magnetic field components produced by coils consisting of straight line or circular current elements. Straight line current elements are counted counter-clockwise about the corresponding coordinate directions. All currents are positive counter-clockwise.

Input variable list

variable name	definition
im	number of increments in x direction.
jm	number of increments in y direction.
km	number of increments in z direction.
dx	"delta x"
dy	"delta y"
dz	"delta z"
x(1)	x coordinate of starting point for incrementing.
y(1)	y coordinate of starting point for incrementing.
z(1)	z coordinate of starting point for incrementing.
da	demagnetizing constant for the model.
xmu	magnetic permeability of free space.
coil	individual coil description.
x1,y1,z1	coordinate of the end points of the straight line
x2,y2,z2	current elements making up the coils.
ccur	coil current.
icoil	number of first coil.
ncoil	number of last coil.
nint	number of interfaces.
mm,nn	dimension of interface array.
xx,yy,zz	interface endpoints.
c1	axial distance of solenoid from the center.
x1	solenoid length.
ri	solenoid internal diameter.
ro	solenoid external diameter.
lay	solenoid number of layers.
ntl	solenoid number of turns per layer.

note:

In order for coons to work properly, ww,w1,w2,must be dimensioned to at least ww(4,nint),w1(ntl),w2(ntl).xx,yy,zz have the same dimensions as ww.

integer out

```
dimension x(50),y(50),z(50),
1x1(8736),y1(8736),z1(8736),x2(8736),y2(8736),z2(8736)
2,confg(18),curt(500),coil(18,28),sum(12,50),xx(4,10),yy(4,10),
3zz(4,10),ww(4,10),w1(8736),w2(8736),ld(50)
common c1,x1,lay,ntl,ri,ro,curc,kk,ii,jj,nc
4 format(1x,2i2)
5 format(2f10.4,3i5,3f10.4,2i2)
10 format(2f10.4,2f12.10)
11 format(3i4,6f5.3)
12 format(3i3)
18 format(3i3,f8.3)
```

```

19  format(3f8.2)
111 format(1x,3f6.2,5x,3f11.2)
113 format(4x,1hX,5x,1hY,5x,1hZ,15x,2hBX,9x,2hBY,9x,2hBZ)
116 format(6x,6h inches,20x,5h gauss)
155 format(/,18a4)
156 format(18a4)
159 format(24x,18a4)
192 format("1",t40,"system summary output")
193 format(//t20,"coil description:",16(/t20,18a4)//)
450 read(1,10,end=420)da,ams,xkt,xmu
c
c  For calculating field inside any coil put the ip equal to the
c  number of that coil.
c
  read(4,4)icoil,ip
  xmp=xmu/(4.*3.1415926)
  read(1,156,end=420) (config(ic),ic=1,18)
c
c  Input spatial description:
c  maximum number of x,y,and z increments,delta x,delta y,delta z
c  corner points of the plot.
c
  read(1,11)im,jm,km,dx,dy,dz,x(1),y(1),z(1)
c
c  calculate and store the spatial coordinates for this calculation.
  do 2000 i=2,im
    x(i)=x(1)-(i-1)*dx
  do 2001 j=2,jm
    y(j)=y(1)-(j-1)*dy
  do 50 j=1,100
    sum(i,j)=0.
    read(1,12)ncoil,inpopt,out
    write(7,159)(config(ic),ic=1,18)
    do 200 nc=icoil,ncoil
      write(6,299) nc
c
c  Corresponding values for each 8 coil set should be read from one file.
c
  if(nc.gt.8)go to 28
299 format(1x,"COIL NUMBER",i10)
  read(1,155)(coil(ic,nc),ic=1,18)
  goto 29
28  continue
  if(nc.gt.16)go to 27
  read(2,155)(coil(ic,nc),ic=1,18)
  go to 29
27  if(nc.gt.24)goto26
  read(3,155)(coil(ic,nc),ic=1,18)
  go to 29
26  read(4,155)(coil(ic,nc),ic=1,18)
  read(4,5)c1,x1,lav,ntl,kk,ri,ro,curc,istepx,istepy
  go to 310
29  continue
  if(nc.gt.8)go to 59
  read(1,18)mm,nn,nint,ccur
  go to 61
59  continue
  if(nc.gt.16)go to 57
  read(2,18)mm,nn,nint,ccur
  go to 61

```

```

57 read(3,18)mm,nn,nint,ccur
61 continue
do 80 j=1,nint
do 80 i=1,4
if(nc.gt.8) goto79
read(1,19)xx(i,j),yy(i,j),zz(i,j)
go to 80
79 continue
if(nc.gt.16)go to 77
read(2,19)xx(i,j),yy(i,j),zz(i,j)
go to 80
77 read(3,19)xx(i,j),yy(i,j),zz(i,j)
80 continue
ntot=mm*nn*nint
call coors(nint,mm,nn,ntot,xx,x1,x2,10)
call coors(nint,mm,nn,ntot,yy,y1,y2,10)
call coors(nint,mm,nn,ntot,zz,z1,z2,10)

```

c
c If the inside field is desired this part will be done defining nn2,mm2.
c

```

if(nc.ne.ip) go to 106
im=0
mm2=mm/2
nn2=1
do 99 n=nn2,nn2
do 99 m1=mm2,mm,mm2
do 99 ipp=4,4
if(m1-2)55,55,56
55 m=1
go to 58
56 m=m1
58 im=im+1
ld(im)=4*nn*(m-1)+4*n+ipp
ldl=ld(im)
x(im)=(x1(ldl)+x2(ldl))/2
y(im)=(y1(ldl)+y2(ldl))/2
z(im)=(z1(ldl)+z2(ldl))/2
99 continue
106 continue
lm=ntot
310 continue
ns=0
do 199 i=1,im
do 199 j=1,jm
do 199 k=1,km
ns=ns+1
write(6,298) ns
298 format(1x,"NO. OF POINT",i10)
if(nc.gt.24)go to 201
bx=0.0
by=0.0
bz=0.0
ll=ld(i)
do 210 l=1,lm
if(nc.ne.ip)go to 105
if(l.eq.ll)go to 198
go to 105
198 write(7,104) i,x1(l),y1(l),z1(l),x2(l),y2(l),z2(l),l
104 format(2x,i2,2x,6(f7.3,2x),i7)
go to 210

```

```

105  continue
      dk=1
      a=(x1(1)-x(i))/39.37
      b=(x2(1)-x(i))/39.37
      c=(y1(1)-y(j))/39.37
      d=(y2(1)-y(j))/39.37
      e=(z1(1)-z(k))/39.37
      f=(z2(1)-z(k))/39.37
197  continue
      u=c*f-d*e
      v=e*b-f*a
      w=a*d-b*c
195  format(1x,"l dd=",i3,2x,6(f7.3,2x,"i=",i3),"l=",i3,2x,"i=",i3)
      r1=(a*a+c*c+e*e)**.5
      r2=(b*b+d*d+f*f)**.5
      rs=r1+r2
      rm=r1*r2
      rdr=a*b+c*d+e*f
      rxr=(u**2+v**2+w**2)**.5
194  continue
      h=(rm+rdr)/rm
      if(h-0.01)2,1,1
1    g=rs/(rm*(rm+rdr))
      goto 3
2    g=((rs)*(rm-rdr))/(rm*rxr*rxr)
3    curm=xmp*ccur*g*10000*dk
      bx1=curm*u
      by1=curm*v
      bz1=curm*w
      bx=bx+bx1
      by=by+by1
      bz=bz+bz1
210  continue
      if(nc.le.24) goto 202
201  call circe(x(i),y(j),z(k),bx,by,bz,br,istepx,istepz)
202  continue
      sum(1,ns)=sum(1,ns)+bx
      sum(2,ns)=sum(2,ns)+by
      sum(3,ns)=sum(3,ns)+bz
      if(nc.le.24) go to 203
      sum(6,ns)=sum(6,ns)+bx
      sum(7,ns)=sum(7,ns)+by
      sum(8,ns)=sum(8,ns)+bz
203  continue
199  continue
200  continue
      write(7,192)
      write(7,159) (confg(ioc),ioc=1,18)
      write(7,193) ((coil(ic,ni),ic=1,18),ni=icoil,ncoil)
      write(7,113)
      write(7,116)
      ns=0
      do 410 i=1,im
      do 410 j=1,jm
      do 410 k=1,km
      ns=ns+1
      write(7,111) x(i),y(j),z(k),(sum(ii,ns),ii=1,3)
410  continue
420  continue
      stop

```

end

c
c This subroutine calculates the field of a solenoids due to circular
c current elements.
c istepx,istepy are the number of wires in x and y direction which
c approximated as one wire.

c
c subroutine circe(xp,yp,zp,bx,by,bz,br,istepx,istepy)
c double precision xk1,xk2,k,e
c dimension r(100),xw(100)
c common c1,x1,lay,nt1,ri,ro,cunc,kk,ii,jj,nc
c pi=3*atan(sqrt(3.))
c cc=.0000002
c a=nt1-1
c do 10 i=1,nt1
c b=i-1
10 r(i)=(ri+b*(ro-ri)/a)/39.37
c aa=lay
c aa=x1/aa
c do 20 i=1,lay
c xi=i
c xi=xi-.5
20 xw(i)=aa*xi
c br=0
c bx=0
c do 30 i=1,lay,istepx
c do 30 j=1,nt1,istepy
c rho=(sqrt(zp**2+yp**2))/39.37
c c=(xw(i)+c1)*kk
c xx=(xp-c)/39.37
c a=r(j)
c xk2=4.*a*rho/((a+rho)**2+xx**2)
c k=pi/2
c e=k
c if(xk2.eq.0)go to 25
c if(xk2.eq.1)go to 30
c xk1=1-xk2
c g0=13.8629436112d-1
c g1=0.96663442590d-1
c g2=3.590092383d-2
c g3=3.742563713d-2
c g4=14.51196212d-3
c g5=.5d0
c g6=124.98593597d-3
c g7=.6880248576d-1
c g8=332.8355346d-4
c g9=441.787012d-5
c h0=4432.5141463d-4
c h1=.626060122d-1
c h2=4.757383546d-2
c h3=1.736506451d-2
c h4=24.99836831d-2
c h5=.9200180037d-1
c h6=40.69697526d-3
c h7=.526449639d-2
c k=g0+g1*xk1+g2*xk1**2+g3*xk1**3+g4*xk1**4+(g5+g6*xk1+g7*xk1**2
c 1+g8*xk1**3+g9*xk1**4)*(log(1./xk1))
c e=1+h0*xk1+h1*xk1**2+h2*xk1**3+h3*xk1**4+(h4*xk1+h5*xk1**2+h6*xk1
c 1**3+h7*xk1**4)*(log(1./xk1))
c br=cc*cunc*xx*1000/(rho*((a+rho)**2+xx**2)**.5)*(-k+(a**2+

```

1rho**2+xx**2)*e/((a-rho)**2+xx**2))+br
25  continue
    bx=bx+cc*curc*10000/(((a+rho)**2+xx**2)**.5)*(k+(a**2-rho**2-
30  1xx**2)*e/((a-rho)**2+xx**2))
    continue
    xs=istepx
    rs=istepr
    br=br*xs*rs
    bx=bx*xs*rs
    by=0
    bz=0
    if(rho.eq.0)go to 40
    theta=atan(yp/zp)
    bz=br*cos(theta)
    by=br*sin(theta)
40  continue
    return
end

c
c  This subroutine calculates the endpoints of wire filaments
c  in a coil. The coil is approximated by a series of quadrilateral
c  interfaces.
c  variable      definition
c  ww(i,)        vertex coordinates for each interface.
c  w1(ind)        first endpoint of filament.
c  w2(ind)        second endpoint of filament.
c  lim           second dimension of ww array.
c
c  subroutine coors(nint,m,n,ntot,ww,w1,w2,lim)
c  dimension ww(4,lim),w1(ntot),w2(ntot)
c  if(m.gt.1.and.n.gt.1) go to 100
c  ind=0
c  if(m+n.ne.2) go to 110
c  write(7,200)
200  format("the filament coordinates are already specified")
c  return
110  if(m.ne.1) go to 120
c  do 40 j=1,n
c  do 40 k=1,nint
c  ind=ind+1
c  w1(ind)=(ww(1,k)*(n-j)+(j-1)*ww(4,k))/float(n-1)
40  continue
c  go to 130
120  do 50 i=1,m
c  do 50 k=1,nint
c  ind=ind+1
c  w1(ind)=(ww(1,k)*(m-i)+(i-1)*ww(2,k))/float(m-1)
50  continue
c  go to 130
100  ind=0
c  do 10 i=1,m
c  do 10 j=1,n
c  do 10 k=1,nint
c  ind=ind+1
c  w1(ind)=(ww(1,k)*(n-j)*(m-i)+ww(4,k)*(j-1)*(m-i)+
1  ww(2,k)*(i-1)*(n-j)+ww(3,k)*(i-1)*(j-1))
2  /float((m-1)*(n-1)))
10  continue
c
c  w2 is generated from w1 so that the endpoints for each coil

```


c are together.
c
130 k=m*n
nn=nint-1
do 20 l=1,k
ll=(l-1)*nint
w2(l*nint)=w1(ll+1)
do 20 i=1,nn
w2(i+ll)=w1(i+1+ll)
20 continue
return
end

Side and Lift Force Coils Magnetic Field

system summary output

coil description:

lift coil x(+) y(-) z(-)
 lift coil x(+) y(+) z(+)
 lift coil x(+) y(-) z(+)
 lift coil x(+) y(+) z(-)
 lift coil x(-) y(+) z(-)
 lift coil x(-) y(-) z(-)
 lift coil x(-) y(+) z(+)
 lift coil x(-) y(-) z(+)
 lift coil 2 x(+) y(-) z(-)
 lift coil 2 x(+) y(+) z(+)
 lift coil 2 x(+) y(-) z(+)
 lift coil 2 x(+) y(+) z(-)
 lift coil 2 x(-) y(+) z(-)
 lift coil 2 x(-) y(-) z(-)
 lift coil 2 x(-) y(+) z(+)
 lift coil 2 x(-) y(-) z(+)

X	Y	Z	BX	BY	BZ
inches			gauss		
5.00	0.00	0.00	0.00	0.00	3210.41
4.00	0.00	0.00	0.00	0.00	2498.65
3.00	0.00	0.00	-0.00	0.00	1827.49
2.00	0.00	0.00	-0.00	0.00	1194.03
1.00	0.00	0.00	0.00	-0.00	589.29
0.00	0.00	0.00	-0.00	-0.00	0.00
-1.00	0.00	0.00	-0.00	-0.00	-589.29

63

ORIGINAL PAGE IS
 OF POOR QUALITY

Drag Coils Magnetic Field

system summary output

coil description:

drag coil 1

drag coil 2

X	Y	Z	BX	BY	BZ
inches			gauss		
5.00	0.00	0.00	-2986.28	0.00	0.00
4.00	0.00	0.00	-2441.84	0.00	0.00
3.00	0.00	0.00	-1862.83	0.00	0.00
2.00	0.00	0.00	-1257.09	0.00	0.00
1.00	0.00	0.00	-633.15	0.00	0.00
0.00	0.00	0.00	0.00	0.00	0.00
-1.00	0.00	0.00	633.15	0.00	0.00

Magnetizing Coils Magnetic Field

system summary output

coil description:
Magnetizing coil 1
Magnetizing coil 2

X	Y	Z	BX	BY	BZ
inches			gauss		
5.00	0.00	0.00	-7258.84	0.00	0.00
4.00	0.00	0.00	-7326.72	0.00	0.00
3.00	0.00	0.00	-7379.74	0.00	0.00
2.00	0.00	0.00	-7417.71	0.00	0.00
1.00	0.00	0.00	-7440.53	0.00	0.00
0.00	0.00	0.00	-7448.14	0.00	0.00
-1.00	0.00	0.00	-7440.53	0.00	0.00

REFERENCES

1. Kraemer, R A, "Low A.C. Loss Superconducting Coils for a Wind Tunnel Magnetic Suspension and Balance System", M.S. Thesis, M.I.T., Sept., 1978.
2. Prey, S W, "A.C. Losses in Interacting Superconducting Magnetic Coils", M.S. Thesis, M.I.T., Sept., 1979.
3. Stephens, T, "Design, Construction and Evaluation of a Magnetic Suspension and Balance System for Wind Tunnels", M.I.T., Aerospace Research Division, TR 136, Nov., 1969.
4. Callarotte, R C, "The Mixed State in Type II Superconductors", Ph.D. Thesis, M.I.T., June, 1967.
5. Stephens, T, and R Adams, "Wind Tunnel Simulation of Store Jettison with the Aid of Magnetic Artificial Gravity", NASA, CR 1955, Feb., 1972.
6. Newhouse, V L, "Applied Superconductivity", Vol II, Academic Press, 1975.
7. "Magnetics", a publication of the IEEE Magnetic Society, Jan., 1977.
8. Sass, A R and J Stoll, "Magnetic Field of a Finite Helical Solenoid", Lewis Research Center, NASA, TN D-1993.
9. Brown, G V, L Flax, E C Itean and J C Laurence, "Axial and Radial Fields of a Thick Finite-Length Solenoid", NASA TR R-170.
10. Hastings, C, Jr., "Approximation for Digital Computers", Princeton University Press, 1955.
11. Stratton, J A, "Electromagnetic Theory", McGraw-Hill, 1941.

12. Way, P, "TABLE Program Modifications", M.I.T. Aerophysics Lab. Internal Memo AR 1031, Nov., 1977.
13. Alishahi, M, "TABLE Program Modifications", M.I.T. Aerophysics Lab. Internal Memo AR 1033, Aug., 1979.
14. Alishahi, M, "Testing Computer Program TABLE", M.I.T. Aerophysics Lab. Internal Memo AR 1034, Oct., 1979.

End of Document